SOVIET PHYSICS USPEKHI VOLUME 5, NUMBER 3 NOVEMBER-DECEMBER 1962

*STRONG-CURRENT PULSE (SPARK) DISCHARGES IN GAS, USED IN PULSED LIGHT SOURCES**

I. S. MARSHAK

Usp. Fiz. Nauk 77, 229-286 (June, 1962)

INTRODUCTION

STRONG-CURRENT pulsed discharges in gases have been thoroughly studied during the past 10—15 years both in connection with new methods of observing processes of very short duration and in view of the urgency of their technical and scientific applications (the production of high-temperature plasma for thermonuclear reactions, pulsed light sources, high-voltage techniques, metal working by electric erosion, switching apparatus, etc.).

Various discharge applications have necessitated specific research programs (for example, high temperature and the associated problems of magnetic plasma confinement in research on thermonuclear reactions; high light yield, compactness, controllability and stability in research on pulsed light sources; intense wear of electrodes in research on electric erosion, etc.). The slanting of the extensive research done in many laboratories towards specific aims has led to the development of several independent and narrow physical disciplines dealing with strong-current pulsed discharges in gases. The contact between these disciplines, which is clearly insufficient at present, is appreciably hindered by the large degree of fragmentation of the published reports and by the almost total absence of review papers. It is the aim of the present article to bridge this gap somewhat by reviewing the research done on the strong-current pulsed discharges used in pulsed light sources. The need for such a review has arisen also in connection with the development of the problem itself. We consider in this article pulsed discharges at pressures close to atmospheric, at voltages from several hundred volts to several tens of kilovolts, with discharge gaps ranging from several millimeters (in inert and molecular gases at a pressure of several atmospheres) to several tens of centimeters (inert gases in narrow tubes at pressures of several hundred mm Hg). The discharges last from 10^{-7} to 10^{-2} second; the energy discharged through the gas gap ranges from 10^{-3} to 10^{5} Joules, and the discharge repetition frequency is from individual pulses to 10^{4} cps.

Even in the case of a stationary arc, an approximate mathematical calculation of all the characteristics is possible only for particular individual discharges (for example, see the papers by Ellenbaas-Heller and Schmitz [212] on discharges in long cylindrical tubes, and also those of Schirmer and Friedrich [163-164] and others [55]. It would be even more difficult to consider in general form all the physical quantities involved in the strong-current stage of the pulse (spark) discharge, which is characterized by a much larger number of parameters.

In this connection, the study of the strong-current stage proceeded primarily via an experimental-phenomenological investigation of the time variation of individual physical quantities. The most important research topics were: a) the electric parameters of the discharge—gap voltage, current strength and density in the discharge, resistance (or conductance) of the discharge channel; b) the expansion of the discharge channel and the accompanying gas-dynamic processes; c) the characteristics of the radiation from the discharge—light intensity, brightness, spectral composition; d) the processes near the electrodes.

The main data on the electric characteristics of discharges were obtained by Rogowski and others [17, 82,84,156-159,161], who determined the rate of "collapse" of the voltage in the gas gap and the current buildup; by Laporte [87], Murphy and Edgerton [36,140], Abramson and Marshak [3,117-119,121,124,127,131] and Vul'fson [215], who observed the existence of a finite resistance in a pulsed discharge with a channel bounded by the wall of the discharge tube, and who established the presence of a limiting current density in bounded and unbounded discharge channels; and by many other later workers [1,6-8,20,24,51,67,80,91,134,142,173,219], who studied the time variation of all the electric characteristics (including discharge power and resistance for various gap and supply circuit parameters. Among the later group of investigations mention can also be made of numerous materials on the electric characteristics of commercial flash lamps [4,5,10,77,120,129,133,141,154,184,205b]. Many papers [6a,67,83,183,209,210,211,212 et al] deal with the electric processes in various circuits that include a spark gap. In [119,121] an attempt was made at an approximate combined calculation of all the parameters of a pulse discharge in a tube during the time when the discharge channel fills its entire cross section. Related to the investigation of the electric characteristics of the strong-current stage of a spark gas discharge are the corresponding studies of pulsed gas discharges occurring in the vapor of a metal wire exploded by an electric current [25,26,30,43,85,128,139,174,181,214].

*The present review is a natural continuation of the review on breakdown of gases at pressures close to atmospheric. [126]

The expansion of the discharge channel was investigated in greatest detail by Mandel'shtam, Abramson, Gegechkori, Drabkina, and Dolgov[2,31,32,63,116], who found an analogy between this expansion and a hydrodynamic explosion accompanied by a short-duration release of a tremendous energy in a narrow plasma channel, an increase in the volume of the heated gas, and propagation of a shock wave. Taylor[182], Drabkina[32], Shao Chi Lin[166], Braginskii[16], and Morgenroth, Hess, Kischel, and Seliger[138] made a mathematical analysis of such a hydrodynamic process, while many other authors [7,21-22a,49,54,65,67,70a,71,79,80,84,91,117,131,146,177-179,197,216] accumulated much experimental material on the velocity and character of the expansion of the gas gap and the supply circuit, and also disclosed specific deviations from the purely hydrodynamic picture, due to the instability of the channel.

The characteristics of the radiation from the discharge were obtained by Laporte and his co-workers [86,88-90,95], Edgerton et al[34,37,39], Bogdanov and Vul'fson[13,14], Marshak et al[121,122,125,131,207,208], Mak[106] and many others[147,149,172,186,213], who investigated the radiation from a discharge bounded by a discharge tube, and also Vul'fson, Charnaya, and Lubin[187,188,190,215,217,218] and Vanyukov, Mak, Muratov et al[107,193-205], who investigated the radiation from an unbounded discharge and demonstrated the existence of a limit on its brightness. Many spectral and temporal characteristics of bounded and unbounded discharges were obtained by Mandel'shtam, Sukhodrev, et al.[112-116,192], Glaser[64-67], Fischer [45-50a], Frungel[59-62], Craggs, Meek, et al.[27-29,110] and many others[9,11,18,73,76-76b,104,111,131,135,141a-143,150,160,162,180,185,205a,213a].

Phenomena on the electrodes of a pulsed discharge were investigated by Froome[56-58], Somerville, Blevin et al.[12,52,175-179], Raĭskii[151,152], Zimin[169], Mandel'shtam, Sukhodrev, and Shabanskii[114,116,121], Zingerman[171], Hermoch[70], Zizka[220], and others[15,33,97-99,100,148,131,206].

II. ELECTRIC CONDUCTIVITY OF DISCHARGE CHANNEL

2.1. Qualitative Picture

At the present time there are two approaches to determining the electric characteristics of a pulsed discharge.* The first[6a,67,82,183,209-212] is principally a mathematical analysis of the variation of the electric quantities in a circuit containing a spark gap, for a specified time variation of the impedance of the spark-gap channel. The second is a direct physical investigation of the processes that determine the electric conductance of the gap in the gas. In view of the emphasis on physics in the present review, we consider in detail the second approach to the problem.

As shown in [126], the buildup of the current density during the course of breakdown is due to a series of avalanche-like processes which go into action successively one after another at an ever increasing speed: these processes are impact ionization by the electrons (α ionization), interactions between α and Γ ionizations (secondary processes at the cathode), effect of a planar space charge on the α and Γ ionizations, interactions between the α ionization, photoionization in the gas itself and the space charge concentrated in the streamer head, etc. A longitudinal electric gradient is established in the plasma channel produced behind the head (or between the heads in the case of simultaneous development of a streamer from the anode to the cathode) in the ionized gas.* This gradient is equal to the ratio of the potential difference across the gap (after subtracting the voltage drops between the heads and the corresponding electrodes; these drops constitute the electrode voltage drops after the channel has grown to the entire length of the gas gap) to the length of the channel. If the discharge power supply has sufficient capacity (low resistance and inductance of the discharge circuit and large supply capacitor) to permit the potential difference on the gap to exceed by many times the sum of the electrode voltage drops, then the most intense avalanche, which is characteristic of the highest ionization in current density, will occur in the channel under the influence of the appreciable longitudinal electric gradient. In view of the considerable degree of excitation and ionization of the gas in the channel and because of the large simultaneous influence of many particles on one another, the various elementary interactions between the atoms, ions, electrons, and photons, can no longer be considered separately in this stage. It becomes meaningful to speak here of a general resultant thermal ionization of the gas or some sort of analog of this ionization in the case of incomplete thermal equilibrium. The avalanche produced in the channel by the longitudinal electric gradient consists of thermal ionization of the

*In addition to the conductance of the channel and its properties as an electric circuit element, one can mention also other electric characteristics of the discharge, such as the controlled and uncontrolled ignition voltage and the discharge-quenching voltage, the delay in the occurrence of the electric current, and the conditions for the deionization of the gap. In the present review, however, we consider only the conductance of the channel, since it is connected with the development of the physical notion of the discharge as a whole. Other electric characteristics are of considerable interest from the technical point of view and are discussed in the specialized literature on pulsed lamps (see, for example, [10,68,77,101,131,132,154,196,219]).

*On going from a diffuse to a contracted discharge structure, more than one channel may be seen to develop in some cases[216]. This obviously is a consequence of the simultaneous occurrence in several regions of the diffuse discharge of conditions that are statistically favorable for the initiation of streamers. The presence of "twin" channels may distort somewhat the gas-dynamic picture of the expansion of the discharge string. However, one should not expect in this case an appreciable difference in the physical properties of the processes or in the electric and optical characteristics of the discharge.

gas, an ionization that increases under the influence of the energy dissipated in the channel and the electric power developed by the discharge. This power increases in turn as a result of the increased current density resulting from the increasing ionization.

This avalanche process can be clearly visualized by considering the mathematical expression for the current density j (which multiplied by the electric gradient yields the power dissipated per unit volume), the degree of thermal ionization x,* and the electric gradient E

$$j = \frac{0.75ne_0^2}{\sqrt{\frac{8}{\pi}kTm}}\, x\lambda E, \tag{1}$$

$$\frac{x}{\sqrt{1-x}} = \frac{0.9}{\sqrt{p_0}}\, T^{3/4} e^{-5850\frac{V_i}{T}}, \tag{2}$$

$$El = U_0 - U_e - L\frac{dI}{dt} - R_b I - \frac{1}{C}\int_0^t I\,dt. \tag{3}$$

Here n —number of gas atoms (neutral or ionized) per cubic centimeter, e_0 and m —charge and mass of the electron, k —Boltzmann's constant, T —averaged gas temperature, which we assume approximately equal to the electron temperature, λ —electron mean free path, p_0 —initial gas pressure, V_i —ionization potential, l —distance between electrodes, U_0 —initial voltage on the supply capacitor, C —its capacitance, U_e —sum of the near-electrode drops in the discharge, I —current in the discharge, L and R_b external inductance and resistance of the discharge circuit, t —time.

Expression (2) shows how fast the degree of ionization increases with temperature (at not too large values of T, for which $5{,}850\ V_i/T \gg 1$ and $x \ll 1$). It is seen from (1) that if E is constant and λ is independent of x (when the terms in the right half of (3) subtracted from U_0 are small and x is so small that the total ion cross section is much smaller than the total atom cross section) the electric power itself, which determines the temperature, increases in proportion to the degree of ionization.

Such a self-exciting or avalanche process leads to an increase in the current density by many orders of magnitude which can be stopped or slowed down, generally speaking, only for the following reasons (or a combination of these reasons):

1) The electric power dissipated in the discharge stops growing because further increase in x leads to a drop in E such that an increase in j becomes impossible. This drop in E may be due either to the characteristics of the external discharge circuit (resistance, inductance, or low capacitance of the supply capacitor) or to an increase of the electrode voltage drops U_e in the case of large j.

2) The increase in current density is greatly retarded by an increase in the degree of ionization and in the total ion cross section, such that the electrons are scattered essentially by the ions and not by the atoms, and λ becomes inversely proportional to x.

3) The temperature stops increasing because the power dissipated in the discharge by the electric current becomes equal to the radiation power, which grows faster with temperature.

Experimental data on the time variation of the electric characteristics (the voltage U on the gas gap and the current I in the discharge, and also various functions of these quantities such as the power, the time rate of the current, etc.) can under certain conditions supplement the foregoing description of the process, which cannot be completed by purely theoretical means since it is impossible to calculate the ionization prior to the establishment of the thermal equilibrium or the energy loss from the channel into the surroundings. To obtain the additional information we must:

a) determine the character and duration of the increase in I and dI/dt and the reduction in U during the nonstationary phase of the "avalanche" process described above;

b) ascertain the actual causes of the termination of this avalanche process and the character of the discharge after the termination.

Generally speaking, it is very difficult to obtain oscillograms of the electric characteristics and thus answer the last question, because even if one of the foregoing factors suspends the growth of the current density and makes the discharge go into a "quasi-stationary state," the current strength should continue to increase rapidly as a result of the channel broadening. For example, in the breakdown of air at atmospheric pressure, the initial discharge channel has a diameter equal to the streamer diameter (~ 0.1 mm [118]). If the avalanche-like growth in the current density j continues in the channel prior to the establishment of the quasi-stationary state, according to rough estimates, for 50 nanoseconds [112,118] and the channel expansion proceeds at shock wave velocity (~ 10^5 cm/sec, which corresponds to a rate of diameter increase of ~ 2×10^5 cm/sec), then during the 50 nanoseconds following cessation of the growth of j, the channel diameter d increases by 0.1 mm, i.e., the current continues to grow, even at constant j,

*As is well known, if we assume T equal to the electron temperature formula (1) can also be used if $e_0E\lambda/1.5kT \ll 2$. It can be shown [117-119] that for spark discharges at pressures close to atmospheric this inequality is reliably satisfied. The Saha formula (2) can also be used [191] if the gas and electron temperatures are equal, i.e., in thermal equilibrium. In highly nonstationary processes, typical of the start of the strong-current stage of the spark discharge, these formulas do not correspond exactly to the actual values of j and x. However, an estimate made in [117,118] and a more careful analysis made in [112] have shown that they are applicable several times 10 nanoseconds after the establishment of the quasi-stationary discharge mode. These formulas can therefore be used for a qualitative description of the processes. It must also be remembered that formula (2) pertains only to singly ionized atoms and that for large T, at which it yields a value of x close to unity, the secondary ionization with a new value of V_i begins to play an important role.

at a rate of the same order as during the avalanche growth of j (it is possible that initially, at small absolute values of d, the rate is even faster).

It follows therefore that in order to solve the foregoing problems by taking oscillograms of the electrical characteristics, the greatest information can be gained in experiments with artificially constricted discharge channels.

If the discharge circuit has appreciable resistance, the avalanche-like increase in the current should, in accord with (3), reduce the voltage across the discharge (the value of $El + U_e$) rather rapidly to the value of the voltage that would be obtained across an arc with a current determined by the value of U_0 and the ballast resistance R_b of the circuit. A voltage variation of this kind is illustrated by curve 1 of Fig. 1. With a negligible active resistance R_b and sufficiently large supply capacitor C, the decrease in voltage across the spark gap, resulting from the vigorous increase in the current strength, should be LdI/dt (L —inductance of the circuit). If L is sufficiently small, to make LdI/dt appreciably smaller than the initial voltage U_0 across the gap at the maximum value of dI/dt, connected with the avalanche-like increase in j and the subsequent expansion of the channel, then the variation of the voltage across the gap should have at the start of the strong-current stage a form shown schematically in Fig. 1 by portion ABC of curves 2 and 3. In the case of an unbounded discharge channel it is expected that any further variation of the gap voltage will correspond to portion CE, which represents a constant capacitor discharge with a prolonged increase in the current strength as a result of the channel expansion. On the other hand, if the channel of the discharge has an artificially confined diameter, which is reached by the instant C, then if the current density j has reached a maximum by that time, the current at that instant should also become maximal. In this case dI/dt should vanish and the voltage on the gap should rise to the point D (this process may not be instantaneous, since the delay in the channel expansion may be gradual and the increase in the gap voltage should cause an additional increase in j). As the capacitor discharge proceeds further, the voltage should follow the path DE_1.

Thus, if the voltage oscillogram of a discharge with unbounded channel has the form ABCE, this should be evidence of the possibility that the current density stops increasing not only because of inadequate power supply (cause 1a), but additionally as a result of one of the other three mentioned causes. On the other hand, if the oscillogram obtained has the form $ABCDE_1$ for a discharge with a channel limited in diameter in some zone, this should prove that it is precisely in this zone that the current density has a limited value. Were such a voltage variation to be observed for a limited diameter of the discharge region near one of the electrodes (resulting from the small area of the uncovered part of the electrode), this would prove the existence of a limit on the current density in this region and the need for increasing the corresponding voltage drop near the electrode in order to obtain larger values of j (cause 1b). If the area of the electrodes proves to exert no influence and the oscillograms obtained when the discharge column is confined by the walls of the surrounding tube have the form $ABCDE_1$, this proves that the principal role is played by causes 2 and 3. The corresponding current oscillograms should permit an absolute estimate of the maximum current density and thereby make more precise the role of each of these two causes.

An artificial increase in the length of the discharge channel (by prior ionization of the gap with an auxiliary voltage source), which is particularly effective in the case of a discharge in an inert gas [132] such as used in tubular flash lamps, or the use of a pulse discharge in the vapor of a long metallic wire previously exploded with current [30,43,75,85,128,139,174,214], permits an appreciable reduction in the initial longitudinal electric gradient in the channel. In the case when causes 2 or 3 are effective, the maximum current density and strength should be appreciably less than for short spark gaps. Accordingly, the portion ABCD of the voltage oscillogram (curve 3) should degenerate in the case of small L into a rather small spike (curve 4 of Fig. 1). After this hardly noticeable spike, the voltage should behave in the manner as on a slowly varying resistance through which a capacitor is discharged.

The voltage across a short spark gap could in principle have a similar behavior, if the inductance of the discharge circuit were so small as to make $LdI/dt \ll U_0$ with the current having a maximum slope as a result of the avalanche-like thermal ionization in the initial channel and subsequent channel expansion.

The variation of the voltage across the discharge should be particularly close to that of a capacitor discharged through a fixed resistance in the case of a constant channel diameter, bounded by walls of a sufficiently narrow discharge tube, such as is characteristic of tubular flash lamps. A discharge of the latter type can therefore be ascribed some constant effective ohmic resistance.

2.2. Experimental Material

2.2.1. Avalanche-like buildup of current density. As long ago as in 1927—1928, Rogowski and his coworkers [156,157] have established that the voltage across a spark gap, fed from a circuit with large ohmic resistance (thousands of ohms) "collapses" immediately after the start of the breakdown, within several tens of nanoseconds (sometimes with a slight interruption lasting about 1 microsecond), from several kilovolts to negligible values approximately corresponding to the voltage across an arc discharge (hundreds of volts). The "collapse" of the voltage

during breakdown was subsequently the subject of many experimental researches. Buss [17], Krug [82], Kohrmann [78], and Kuhn [84] studied the voltage ledge —the interruption in its vigorous drop, occuring at a level 60—85 per cent of the initial voltage and lasting several tenths of a microsecond. According to ideas developed in [126], this ledge is connected with the existence of a short-duration diffuse glow discharge phase, which in some cases (in the case of slight overvoltages) precedes the formation of the contracted channel of highly-ionized plasma. In all the foregoing investigations except the last, the ledge was observed with the discharge fed from a circuit with large active resistance. The current strength in this phase of the discharge was insignificant, about 1 ampere. Mezhueva, Stekol'nikov, and Efendiev [134], who made a special study of the collapse of the voltage in discharges fed from circuits with low active resistance and with inductance 0.05—2.9 μH, and also Abramson and Marshak [3], who used a circuit with negligible resistance and with an inductance of about 0.1 μH observed no glow-discharge ledge. Nor is the presence of a ledge mentioned in the paper by Abramson and Gegechkori [1], where the circuit resistance was negligibly small and its inductance varied between 2 and 64 μH. However, a later investigation by Kuhn [84] has demonstrated the existence of a corresponding ledge in the case of breakdowns at small overvoltages, even in the case of negligibly small active circuit resistance and an inductance of 3.6 μH, at which the discharge current reaches 10—100 amperes at the end of the ledge.* Increasing the overvoltage to several per cent (the larger the gas pressure and the longer the gap, the smaller the increase) leads to a decrease in the duration and then to a complete disappearance of the ledge, that is, to the formation of a contracted channel with rapidly developing thermal ionization in the earlier phase of the breakdown (before the current in the diffusion discharge exceeds a value of about 10^{-2} A). The question of the dependence of the ledge on the supply-circuit power and the possibility of its appearance at much lower circuit inductances than used by Kühn still remains open.

All the cited investigations, and also the work by Andreev and Vanyukov [7] provide an approximately equal estimate of the duration t_{col} of the steepest portion of the voltage collapse (10^{-8} sec). At the same time, the actual values given by different authors for this quantity differ by several times. Values from

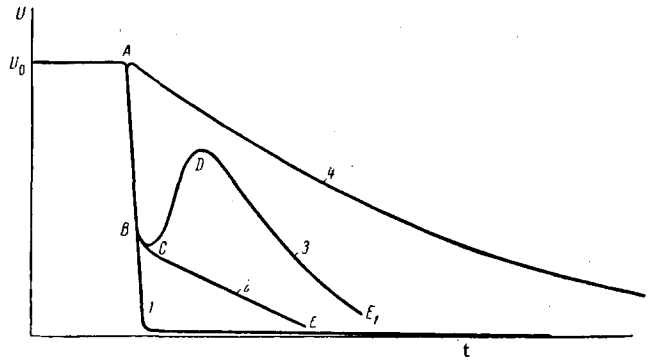

FIG. 1. Expected variation of voltage in a pulse discharge, fed from a discharge circuit with large active resistance (1), with sufficiently small resistance and inductance and large capacitance (2—case of unbounded channel, 3—channel of limited diameter), and also in a discharge with artificially increased distance between electrodes (4).

1.5 to 17.6 nanoseconds were obtained in [134] for discharges in air at atmospheric pressure, and the authors of this paper note the large scatter in the values of t_{col} from experiment to experiment. They also noted the existence of several "resonant" initial voltages on the gas gap, between which t_{col} decreases seemingly by a factor of several times compared with the usual $t_{col} \sim 10$ nsec, obtained for the same circuit at different values of U_0. The occurrence of a "resonance" and the scatter in the values of t_{col} was not confirmed by other investigators; it can be assumed that they are due to experimental errors.*

Kuhn later [84] obtained $t_{col} = 30$ nsec for air at atmospheric pressure and 100 nsec at 250 mm Hg. For hydrogen it is approximately one-third as large as for air, although the slight reduction in the voltage preceding the collapse has an appreciably more pronounced character for hydrogen. Kuhn relates this with the smaller initial electric gradient in the breakdown in hydrogen and accordingly with the slower release of energy needed for the start of thermal ionization in the discharge. Figure 2 shows curves for the power dissipated in the discharge [84], obtained by taking simultaneous oscillograms of the

*Kühn advances the opinion that so strong a current, and also the growth in the current which he noticed during the time of the ledge contradict the assumed existence of the Townsend discharge mechanism in this phase. However, either one or the other can be derived completely by making use of the calculations of Davidson (see [126]), who started from the notion that the Townsend α and Γ ionizations are acted upon by the space charge, that is, essentially within the framework of the Townsend mechanism (without the notion of contraction of the channel and thermal ionization).

*The errors could be due, for example, to the use of an igniting spark, the position and intensity of which could cause the main discharge to develop under different effective overvoltage conditions. One should note at the same time a few other inaccuracies in [134], where the authors negate the previously observed [3] transition from a steep voltage curve to a gently sloping one, and at the same time give extensive quantitative data on the level of this transition (the quantity "K"); they speak of an ambivalent influence of the electrode shape on "K" and at the same time of an increase in "K" for pointed electrodes; the data on the effect of the inductance and capacitance of the circuit on the period T of the natural oscillations of the voltage contradict the classical formula $T = 2\pi\sqrt{LC}$; what passes for mathematical analysis of the problem are calculations of the current and the energy in the spark erroneously based on representing the voltage oscillogram by an exponential curve, which differs from the oscillogram in the most important region of large t by a factor of several times.

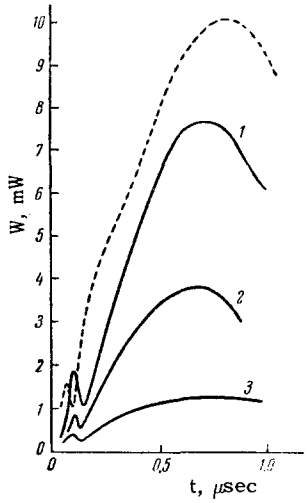

FIG. 2. Power dissipated in the discharge for breakdown in air (dashed curve, pressure p = 750 mm Hg, U = 35.3 kV) and hydrogen (solid lines). 1 – p = 1500 mm Hg, U_0 = 32.5 kV; 2 – p = 1000 mm Hg, U_0 = 25 kV; 3 – p = 500 mm Hg, U_0 = 13.5 kV, C = 0.06 μF, L = 3.6 μH. Distance between electrodes l = 11.7 mm.[84]

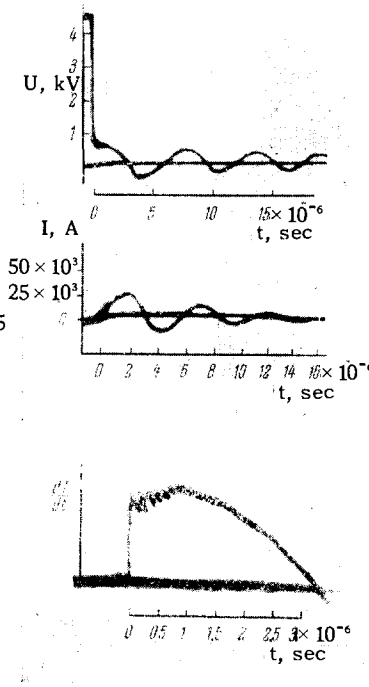

FIG. 3. Typical oscillograms of U, I, and dI/dt for a discharge with unbounded channel. Air, p = 760 mm Hg; l = 1.5 mm, C = 6 μF, U_0 = 4.5 kV, L = 0.16 μH.[3,117]

current and the voltage; these curves confirm that the same amount of power is obtained for hydrogen at twice the pressure.

Andreev and Vanyukov[7], who worked with a very low discharge-current inductance (about 10 nanohenry), estimated the time of vigorous growth of current density to be about 6—8 nanoseconds.

Even shorter voltage-collapse times are obtained at larger over-voltages on the spark gap. Fletcher[53] and Rose[161] have established that at an overvoltage of several hundred per cent the duration of the entire breakdown process, from the start of the ionization to the completion of the collapse, amounts to fractions of a nanosecond. Rose, who worked with short spark gaps (0.03—0.11 mm) in a circuit with very low capacitance (130 pF) and negligible inductance (~ 0.6 nH) at a voltage front 0.75—2.5 kV/nsec steep and maximum overvoltages up to 300 per cent, found that the time of formation of thermally ionized plasma may amount to 0.2 nanosecond and apparently this small quantity is still not the limit.

Thus, there is still no complete picture of the dependence of the duration of the avalanche-like growth of current density and the associate collapse in voltage across a spark gap as a function of the parameters of the gap and the spark circuit.* However, the available experimental material is in full agreement with the previously mentioned tentative calculations[112,117,118], in which estimates were made of the time required for the degree of ionization to reach several per cent under static breakdown conditions (we shall see later on that this value of x corresponds to the cessation of the avalanche-like growth in the current density), the estimate being on the order of several tens of nanoseconds. Under pulse breakdown conditions with large overvoltage and small discharge-gap inductance, this time should naturally be much shorter.

2.2.2. Cessation of avalanche-like growth of current density. The cessation in the growth of the current density at the instant when the voltage collapse terminates, in a discharge with large active balance resistance R_b, should be related principally to cause 1a—the decrease in the longitudinal electric gradient owing to the characteristics of the external discharge circuit. At this instant the discharge does not differ principally from an ordinary arc, although it is characterized by increased densities of the currents (~ 10^4 A/cm^2) and of the gas. During the succeeding instants of time the discharge channel broadens and the densities of the current and of the gas come into agreement with the ordinary arc values. The discharge resistance decreases, but since it is already appreciably smaller than R_b immediately after the collapse, this hardly influences the current strength. The entire process as a whole corresponds to the scheme developed in the description of curve 1 of Fig. 1.

A similar picture is observed in the case when the circuit has a low resistance and a considerable reactance[1,3,67,117]. In this case the gap voltage "collapses" during the course of the avalanche-like increase in the current density to a value 200—300 volts, after which its further variation, as well as the variation of the current, comes rapidly into agreement with that obtained in a strong ac arc fed from a LC circuit. In this case the factor determining the termination of the growth of the current density is undoubtedly cause 1a, although there is a short tran-

*It should be pointed out that [161] contains a reference to an unpublished work by Mainck, who investigated breakdowns without over-voltages, also with very small capacitance (113-140 pF) and inductance (1.8-5.8 nH) in the supply circuit. The collapse times turn out to be in this case greater than 0.8 nsec (no upper limit is given), which can be regarded as an additional indication that the rate of the collapse increases with decreasing inductance.

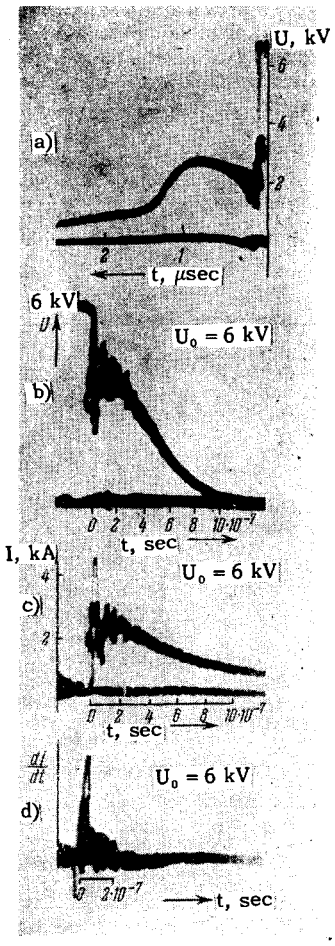

FIG. 4. Typical oscillograms of U, I, and dI/dt for a discharge in a capillary (air, 760 mm Hg). a) C = μF, U_0 = 6.8 kV, L = 0.16 μH, capillary diameter d = 0.6 mm, l = 3 mm; b)–d) C = 0.25 μF, U_0 = 6 kV, L = 0.08 μH, d = 0.2 mm, l = 5 mm.[3,117]

sition period between the instant that the "collapse" terminates and the ordinary arc discharge is established, in which the channel broadens.

As shown in [7,8,117,3], entirely different processes occur in a gas breakdown at visibly small external discharge-circuit resistance, low inductance, and high capacitance. Figure 3 shows typical oscillograms of the voltage, current, and derivative of the current with respect to time, obtained for breakdown in air. In this case the course of the voltage U agrees well with curve 2 of Fig. 1, which pertains to a discharge in which the limiting current density is attained during the "collapse" time, with a considerable voltage U_i remaining on the discharge, and the current strength continues to increase after the "collapse" at almost constant rate dI/dt, owing to the subsequent expansion of the channel. The increase in $U_0 - U$ past the maximum of dI/dt is obviously connected with the discharge of the capacitance which by then is already appreciable ($\frac{1}{C}\int_0^t I\,dt$ becomes comparable with $L\,dI/dt$). The voltage U_i remaining on the gap by the instant of termination of the "collapse," increases in accordance with the experimental data with decreasing inductance of the discharge circuit and with increasing U_0 and increasing distance between electrodes (this dependence of U_i on the parameters agrees with the notions regarding the limitation on the current density and the mechanism governing the expansion of the channel—see Sec. 3.2). Experiments to determine the reason for the existence of a limiting current density by limiting different regions of the discharge have shown that the limitation of the cathode working surface or the anode working surface (the corresponding electrode was almost completely coated with insulating material, so that only about 0.05 mm^2 of metal surface was exposed) does not lead to an appreciable change in the form of the oscillograms. This proves that the current density is not limited in the regions near the electrodes (values on the order of 4×10^7 A/cm^2 are obtained, in accordance with work on the determination of the current density in the cathode and anode spots)[12,23,24,33,56-58,175,176], and that the large potential difference between the electrodes after the termination of the collapse is not concentrated in the near-electrode drops (cause 1b). To the contrary, the limitation of the discharge column by the walls of the surrounding capillary tube leads to oscillograms of an entirely different type (Fig. 4). In this figure the voltage variation agrees well with curve 3 of Fig. 1, which pertains to a discharge in which maximum current density is reached after the "collapse" of U, and the maximum current is also reached after the channel fills the internal cross section of the capillary. A similar form is exhibited also by oscillograms of I and dI/dt. With decreasing diameter of the capillary, the saddle BC (Fig. 1) becomes narrower and the hump D becomes higher.

Thus, experiment has confirmed the presence of a certain limiting "saturation current density" j_{sat}, determined by the phenomena in the discharge column (possible causes 2 or 3). A summary of the quantitative estimates of j_{sat} and the corresponding value of the electric gradient E (without account of the voltage drops near the electrodes) and the resistivity $\rho = E/j$ of the plasma in the discharge column, obtained from different experimental data on current and voltage oscillograms (or equivalent other data) and on the column diameter (the capillary diameter or the diameter of the channel measured by high-speed photography) is given in Table I.

Table I shows the following: 1) the values of j_{sat} and ρ, obtained from the experimental data of various workers, for an unbounded channel, have the same order of magnitude, although they differ by a factor of several times, which can be ascribed to different methods used to measure the channel width. This order of magnitude agrees with the one obtained for discharges with bounded channels, although the values of ρ for an unbounded channel lie on the average somewhat lower than those for a discharge in a capillary; 2) a decrease in ρ and an increase in j_{sat}

Table I. Summary of experimental electric characteristics of powerful discharge after "collapse" of the voltage

Author	Reference	Gas	Pressure, atm	Discharge length, mm	Capillary diameter, mm	L, μH	j_{sat}, 10^3 A/cm²	E, V/cm	ρ, 10^{-3} Ω-cm
1. Abramson, Marshak	3	Air	1	5	0.2—0.6	0.1	60	6000	1
2. Fitzpatrick, Hubbard, Thaler	51	»	1	4	0.3	0.01	17	2500	1.5
3. Ogurtsova, Podmashenskiĭ	142, 143	»	1	10	2	1.5*	4	1000	2.5
4. Marshak	117, 118	»	1	3	—	0.1	30	6000	2
5. Abramson, Gegechkori	1, 63	»	1	3	—	2—64	1.2—4	430—1270**	4—2.7
6. Glaser, Sautter	67	Argon	0.5	47	—	0.9	0.1	200	20
7. Komel'kov, Parfenov	80	Air	1	30	—	0.07	90	6000	0.7
8. Kuhn	84	»	1	11.7	—	3.6	0.5—13	1000-4000	20-3
9. Andreev, Vanyukov	7, 8	»	1	8.4	—	0.015	20—50	6000—15000	3
10. Marshak	131	Xenon and argon with hydrogen	3	5	—	0.01—0.08	40	5000	1.3

*Artificial line made of four 100 μF capacitors spaced by 1.5 μH inductances.

**Data on the dependence of the gap voltage on the length were used to estimate the near-electrode drops, which were taken into account in the calculation of E.

are observed with increasing E; 3) the type of gas hardly affects the values of ρ and j_{sat}.

It is advantageous to add to the data of Table I the extensive experimental material on electric characteristics of tubular flash lamps. In these lamps the initial narrow discharge channel, produced by an auxiliary high-voltage pulse, usually is capable of filling more or less uniformly the entire inner cross section of the discharge tube after several microseconds [91]. If the supply capacitor has a sufficiently large capacitance, the time of channel expansion is negligibly small compared with the remaining duration of the discharge, during which the characteristics of the channel change quite slowly and the discharge can be regarded as quasi-stationary.

Being an analog of the short spark discharge in air with a channel bounded by the capillary walls, which we considered above, a discharge in tubular flash lamps has the following essential distinguishing features:

1) It occurs in inert gases, for which the Ramsauer effect is characteristic [153], namely the small cross section with which atoms scatter electrons with velocities corresponding to a temperature of about 10,000°K. Consequently, the total ion cross section in such a discharge begins to exceed the total cross section of the atoms even at relatively low degree of ionization ($x \sim 10^{-4}$) [119]. Further increase in x causes electron scattering by the ions and not by the atoms to assume a predominant role, and this causes the direct dependence of the current density on the degree of ionization to disappear at $x \sim 10^{-4}$ (cause 2 of the possible slowing down in the vigorous growth of j).

2) Since an auxiliary high-voltage pulse is used for the ignition (a procedure particularly effective in inert gases [126]), the length of the discharge channel in tubular flash lamps is artificially increased by one or two orders of magnitude (compared with a spark discharge in molecular gases for the same supply voltage). By the same token, the initial longitudinal electric gradient in such tubes is appreciably decreased. As indicated in Sec. 2.1, one can expect here lower maximum current density and current strength, limited by causes 2 and 3. These reduced limiting values can be attained at relatively large inductance and resistance in the discharge circuit.

3) Relatively low values of the electric gradient and current strength correspond to so low a value of electric power dissipated per centimeter of discharge channel, that the power can be applied for a considerable time to the walls of the discharge tubes without damage. This makes it possible to increase the capacitor rating and thereby increase the duration of the quasi-stationary discharge in tubular tubes by several orders of magnitude compared with the duration of a short spark discharge in a capillary. By the same token, a detailed investigation of this discharge becomes much easier.

The very first experimental data on the electric characteristics of tubular flash lamps (Table II) have

Table II. First (essentially time-averaged) data by certain authors on the resistance of tubular flash lamps, recalculated for ρ by means of formula (4)

Author	Reference	Gas	Pressure, mm Hg	r, mm	l, mm	E*, V/cm	$\rho \cdot 10^2$, Ω-cm
1. Laporte . .	87	Neon	5	3	100	200	0,9
2. Laporte . .	87	Argon	5	3	100	200	1,3
3. Murphy and Edgerton . .	34, 35, 140	Argon, xenon	50—300	3,5—7	100—300	175	1.1—3
4. Vul'fson . .	215	Neon, argon, krypton	5—10	0.8—5	50—500	30—130	3
5. Carlson and Pritchard	19	Xenon	100	2.2	400	50	3
6. Warmoltz and Helmer	205b	"	200	2	200	200	1.6
7. Aldington and Meadowcroft	4, 5	"	60	5.5	460	44	1.5
8. Meyer	133	Argon	200	5	800	100	1.7—4,2
9. Glaser and Sautter	67	Xenon	190	2	300	100	4,5
10. Chesterman and Glegg	20	"	200	1,5	128	80	1
11. Ando and Matsuoka	6	"	50—300	2,5	150	17	2,6
12. leCompte and Edgerton	91	"	300	2	76	118	1,14

*This column lists, for most investigations, the initial values of the gradient without account of the drops near the electrodes. Only for the investigations of Chesterman and Glegg and of leCompte and Edgerton, in which low capacitances only slightly discharged by the instant when the discharge tube was filled with plasma were used, is the instantaneous value of E given for the maximum current strength.

shown that the variation of the voltage in such tubes, for the customary small values of R_b and L of the discharge circuit, is similar to curve 4 of Fig. 1, which in turn approximates an exponential with exponent $-t/RC$, where C is the supply capacitance and R is the resistance of the discharge column, calculated from the formula

$$R = \frac{\varrho l}{\pi r^2} \qquad (4)$$

(l —distance between electrodes, r —internal radius of the tube, ρ —a quantity which can be called the resistivity of the discharge column, and which is approximately the same for different tubes and different supply conditions). For these tubes, the values of ρ are close to one another and exceed by an order of magnitude the values of ρ for short discharges, as listed in Table I.

The absence of a noticeable voltage "collapse" on the oscillograms of the discharge in tubular flash lamps follows from the estimate of the rate of the current force ($\sim 10^7$ A/sec for an avalanche-like increase in j to $\sim 3 \times 10^3$ A/cm^2 in a channel of 0.2 mm diameter within a time $\sim 10^{-7}$ sec; 5×10^7 A/sec in the expansion of a channel with about 1 mm diameter at a rate of 500 m/sec [21,91]) and the usual inductance L and resistance R_b of the discharge circuit (~ 1 μH, 0.01 Ω). Accordingly, LdI/dt and R_bI are on the order of 10 volts and thus negligibly small with the voltages customarily used for flash lamps. They must therefore produce a hardly noticeable spike on the voltage oscillograms, similar to that shown on curve 4 of Fig. 1.

At the same time, the qualitatively similar character of a pulse discharge in a tubular flash lamp and a short spark discharge in a capillary tube is illustratively confirmed by experiment in the case when the former are fed from circuits with considerable values of the external L and R_b, at which LdI/dt and R_bI become comparable with U_0. Thus, for example, in [67], voltage oscillograms similar to curve 3 of Fig. 1 were observed when an inductance of 3300 μH was connected in series with the tubular lamp. In [127], a ballast resistance of 48 Ω was connected and the voltage oscillograms were similar to curve 1 of Fig. 1.

Analogous data can be obtained also for still another form of pulse discharge with artificially lengthened channel, namely a discharge in the vapor of an electrically exploded metallic wire. Even the first researches on the electrical characteristics of such a discharge [3,117,214] have confirmed that the voltage in this discharge has a variation similar to curve 4 of Fig. 1. Later work by Sobolev [174], Kvartzkhava, Plyutto, Chernov, and Bondarenko [85], Muller [43,139] David [30], and Marshak [128], in which the ignition and expansion of the channel of a pulsed gas discharge in metal vapor and its electrical characteristics were investigated, have shown that this discharge is quite similar to that occurring in tubular flash lamps. For example, it is seen from the Toepler pictures (obtained with a Kerr shutter) of [139] that the gas discharge occurs in the form of a thin glowing string approximately 2 microseconds after the explosion of the copper wire.* By that time the already highly

*According to Sobolev [174], if a tungsten wire is used, the gas discharge may begin prior to complete evaporation of the wire, in view of the breakdown of the surrounding gas in parallel with the wire. The way for this breakdown is paved by the very intense thermionic emission of the high-melting-point wire which is heated

rarefied metal vapor fills a cylinder of approximately 6 mm diameter, contained, as if in a tube wall, by a rather dense shock-wave front. After about 3 more microseconds the gas-discharge string fills the entire cylindrical cavity inside the front of the shock wave, the diameter of which has increased to about 8 mm. A comparison of the oscillographic data obtained in [128] on the current and voltage in a pulsed gas discharge in metal vapor with the corresponding data on the expansion of its channel has disclosed that the average resistivity of the discharge plasma, ρ, is approximately equal to 0.008 Ω-cm at an average electric gradient $E \sim 250$ V/cm, regardless of the type of metal and of the wire diameter. Thus, under conditions of discharges with artificially lengthened channels, the value of ρ has the same order of magnitude in the case of an unbounded discharge in vapors of an exploded wire, as in the case of a confined discharge in a tube with inert gas.

2.2.3. General character of the dependence of ρ on E. A detailed investigation of the dependence of the instantaneous value of the resistivity ρ of the discharge plasma, defined by (4), on the structural characteristics of the tube and on the parameters of the supply circuit has been made in [124,127,131]. Figure 5 shows samples of the discharge volt-ampere characteristics obtained in these investigations. The individual branches of the characteristics with positive slopes (pertaining to the quasi-stationary discharge) merge at different values of C and U_0 into one common line. This proves that there exists for each tube a single function $\rho = f(E)$, which is not influenced by the preceding state of the plasma. The portion of this line with nearly constant ratio U/I (constant resistance of the tube) describes the fundamental part of the discharge, during which 80—90 per cent of the energy from the capacitor is dissipated in the tube. Investigations have shown that the resistance of the tube in the case of a quasi-stationary discharge deviates from a quantity corresponding to a unique function $\rho = f(E)$ in only one case—in the earlier stage of discharges, if an appreciable ballast resistance is connected in series with the circuit. A calculation of the heat flow through the walls of the tube [127] shows that in this case the discharge should not fill the entire cross section of the tube within a certain time (which increases with increasing R_b). By the same token, the anomalous values of ρ, calculated from (4) are due to the fact that this formula is not applicable.

Figure 6 shows several plots of the dependence of ρ on E, obtained by corresponding recalculation of the lines, into which the branches of the volt-ampere characteristics with positive slope merge. Curves I—V and VIII pertain to tubular flash lamps with ordinary relatively broad discharge tubes, while curves VI and VII pertain to lamps with capillary discharge tube. In addition, we show here curve IX, obtained by recalculating the experimental values of the voltage U_l existing on the lamp immediately after cessation of the sharp voltage decrease, which is brought about in the case of large R_b by the presence of different ballast resistances in the discharge circuit. The corresponding current strength was calculated here from the formula $I_l = (U_0 - U_l)/R_b$. The last figure gives a patently overestimated value of ρ, which goes over in the later instants of time into those of curve VIII, the faster, the smaller R_b or the larger U_0.

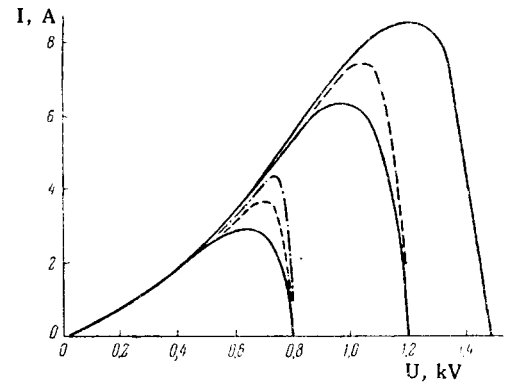

FIG. 5. Samples of volt-ampere characteristics. Xenon, p = 100 mm Hg, l = 7 cm, r = 0.17 mm; —— C = 0.1 μF, – – – 0.25 μF, –·–·– 0.5 μF; U_0 = 0.8, 1.2, and 1.5 kV.[131]

It follows from curves I—V that a practically unique functional connection between the instantaneous values of ρ and E exists not only for each specific tube, but also for similarly filled tubes of different (not too small) length and with different discharge-tube inside diameters ranging from 2 to 8 mm. Analogous measurements for lamps with discharge tubes of the same dimensions but with different gases have shown [124] that substitution of xenon for krypton increases ρ by merely about 15 per cent, and substitution of argon decreases ρ by about 10 per cent. A decrease in the pressure from 100 to 25 mm Hg decreases ρ by only 10—20 per cent.

A comparison of the most accurately measured values of ρ for lamps with r = 1 and 2.3 mm (curves I and II) shows that ρ increases somewhat (by about 20 per cent) with decreasing diameter. The increase in ρ with decreasing r in the region of small E is confirmed by the course of the curves VI and VII, obtained in a different investigation [131] for rather narrow (r = 0.25 mm) capillary lamps. At the same time, in the region of large E ($\gtrsim$ 100 V/cm), the difference between ρ for capillary and for broader lamps becomes small.

The less accurately measured curve VIII lies sufficiently close to curves I—IV to assume the discrepancy between them to lie within the limits of experimental

to a high temperature. Although the subsequent development of the discharge differs somewhat from that in vapor of a more volatile wire (the tungsten vapor expands slowly within the cylindrical shock wave), this should not influence greatly the electrical characteristics.

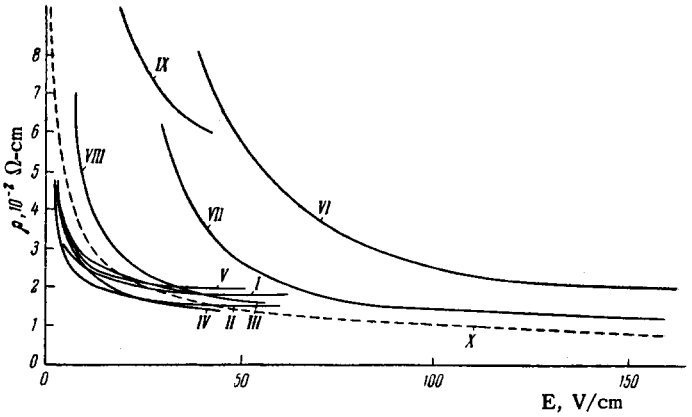

FIG. 6. Curve showing the dependence of ρ on E for tubes with different internal discharge-tube diameters and different filling gases.

Number of curve	I	II	III	IV	V	VI	VII	VIII	IX	X
l, cm	50	50	29	36	36	7	7	100	100	Empirical function $\varrho=\frac{0.1}{\sqrt{E}}$
r, mm	1	2.3	3.3	2	3.8	0.25	0.25	7	7	
Gas	Kr	Kr	Kr	Kr	Kr	Xe	Xe	Xe	Xe	
p, mm Hg	100	100	100	100	100	600	100	120	120	
R_b, Ω	0	0	0	0	0	0	0	0	0.67–48	

error. This indicates that the practically unique functional dependence of ρ on E, referred to in the discussion of curves I—V, apparently is obtained also when the tube inside diameter exceeds 8 mm, at least up to 14 mm.

LeComte and Edgerton[91] correlated the discharge-channel resistance in a tubular flash lamp with the area of its cross section, determined by high speed end-view photography of the channel. This correlation was made for different instants of channel expansion and of the subsequent attenuating pulsation of its diameter, due to reflection of the compression waves from the wall tubes, and showed that the channel resistance remains strictly proportional to the reciprocal of the channel cross section area, within the limits of experimental accuracy, so long as the voltage on the supply capacitor does not drop considerably. By the same token they demonstrated that a unique value of resistivity ρ for a given gradient E is a property not only of lamps with different tube diameters, once they become uniformly filled with plasma over their entire cross section, but also in the same tube at different channel diameters, with the cross section of the tube not completely filled.

We thus reach the conclusion that it is advantageous to introduce some universal function $\rho = f(E)$, which could be used in most cases, with a tolerable degree of error, to calculate the instantaneous resistance of the steady-state quasi-stationary discharge in any tubular flash lamp with arbitrary dimensions and arbitrary gas content. Values of R appreciably differing from the thus calculated values should be observed only in very narrow capillary lamps at relatively low values of E (below 100 V/cm), and also for lamps fed through a ballast resistor immediately after cessation of the sharp voltage decrease and establishment of the quasi-stationary discharge. Of course, much higher values of R should also be obtained in tubes in which the discharge channel does not have time to fill the entire cross section of the discharge tube, owing to the small capacitance of the supply capacitor.

From Fig. 6 and from the foregoing experimental data it follows that for a rough estimate of the effective resistance of a xenon flash lamp with not too narrow a discharge tube, under the most frequently encountered initial electric gradients ~ 50 V/cm, we can use a universal value $\rho = 0.02\ \Omega$-cm. The corresponding value for krypton lamps is $\rho = 0.017\ \Omega$-cm. For a more accurate calculation of the instantaneous resistance of tubes in a broader range of variation of the electric gradient it is necessary to take in place of a constant value of ρ a value which decreases somewhat with increasing E. As can be seen from curve X of Fig. 6, one can choose as a suitable function the empirical formula

$$\varrho = \frac{0.1}{\sqrt{E}}. \tag{5}$$

The empirical relationship $\rho = f(E)$, determined from data on the instantaneous resistance of tubular flash lamps during the stage of quasi-stationary discharge and extrapolated to the region of larger E can be set in correspondence with the data given in Sec. 2.2.2 on the resistivity of the plasma of a short spark discharge and a discharge in the vapor of a metal wire exploded by current, after the saturation current density has been established. Figure 7 shows a plot of the function (5) in this region, as well as the points corresponding to the experimental data given in Sec. 2.2.2. In view of the uncertainty in the measurement of the diameter

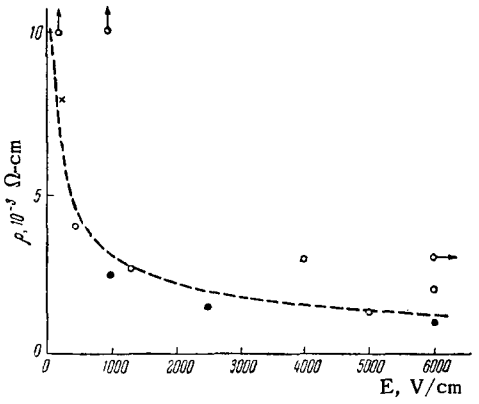

FIG. 7. Comparison of the empirical relation (5) with the experimental data for a short spark discharge and for a discharge in the vapor of a wire exploded by current. Circles – short spark discharge (black circles – in capillary, light circles – with unbounded channel), cross – discharge in wire vapor.

of an unbounded discharge and other measurement errors, formula (5) can be regarded as satisfactorily representing the experimental data with respect to the resistivity of the plasma also in the case of the strong-current (quasi-stationary) states of a short spark discharge and a discharge in vapor of wire exploded by current.

As is well known tubular flash lamps can be fed, in view of their rising volt-ampere characteristic, not only from a capacitor, but also from other voltage sources. Single flashes can be obtained, for example, by feeding the lamps from an ac power line, which produces in the tube a discharge that ignites near the maximum of the voltage and is extinguished when the voltage passes through zero [74,123,129]. Compared with a capacitor discharge, such a discharge is characterized by a much greater duration (about 1/200 sec for a 50 cps line) and an entirely different time variation of the voltage (nearly sinusoidal). Nonetheless, oscillograms taken of the current and voltage of such discharges have shown that soon after the ignition of the lamp its resistance can be calculated with sufficient accuracy by means of formulas (4) and (5). This proves once more the universal character of the physical relationships represented by these formulas.

In fact, an analogous discharge takes place also in the recently announced tubular xenon continuous-glow lamps, rated several times 10 kW. [96,102,103,105,130,130a,165] Unlike the single flashes of the small flash lamps fed from the ac line, in which the discharge is extinguished when the voltage drops to a low value (in view of the negative energy balance in the narrow discharge tube [126,132]), in superpower lamps of large diameter the gas does not have a chance to deionize during the time that the voltage goes through zero. Therefore after the voltage polarity is reversed, the current continues to flow through the tube, but now in the opposite direction. Thus, discharges similar to the pulsed discharges in the capacitorless supply take place in the lamp at double the line frequency. Because of the large surface of the quartz discharge tube and because forced cooling is used in some cases, the tube becomes capable of dissipating the power delivered to it under prolonged operation conditions. Like the tubular flash lamps, these lamps have a definite effective resistance, and unlike different gas-discharge lamps can operate without a ballast to limit the current. Experiment, as well as calculation [55,130,163,164,212] show that at the power concentration prevailing in these lamps the discharge channel fills only part of the tube cross section. Consequently, in calculating the lamp resistance, it is necessary to substitute in (4) the quantity ρ/θ^2 in lieu of ρ, where $\theta \cong 0.5$ is the ratio of the channel diameter to the internal diameter of the tube. Instead of formula (5), which, as can be seen from Fig. 6, gives excessive values of ρ in the region $E < 10$ V/cm, the following dependence on the electric gradient holds for these tubes, with satisfactory accuracy:

$$\frac{\rho}{\theta^2} = 0.065 p_0^{1/2} r^{-1/2} E^{-3/2}. \qquad (6)$$

This formula pertains both to the effective and to the instantaneous values of ρ, θ, and E, calculated from the current and voltage oscillograms and from the sweep photographs of the channel width. They also agree with the increased values of ρ at the first instants of the condensed discharge in the flash lamps with a series ballast resistance (plot IX of Fig. 6).

Many attempts at an approximate theoretical calculation of the electric characteristics of a discharge with high degree of ionization of the gas in the channel have been published. In most of these, certain parameters were assumed specified on the basis of experimental material. Thus, for example, in the chronologically first paper of Mohler [137], in which the resistivity of the column of a strong-current stationary cesium low-pressure discharge was calculated, the losses on the walls were estimated from the experimental values of the ion current on the wall, and the radiation (also on the basis of an experimental estimate) was assumed to be negligibly small. In [118] the diameter of the channel of an unbounded discharge was estimated from experimental data and the radiation power was set equal quite crudely to the radiation power of an absolutely black body of equal dimensions. In [215] experimental values for the discharge power were used, while in [67] the discharge temperature was estimated from the radiation characteristics. Only in [16,119,163-164] were attempts made for a combined theoretical calculation of all physical parameters of the discharge, in the first of these papers for a short powerful spark, in the second for a discharge in tubular flash lamps, and in the third and fourth for the case of a discharge in powerful tubular continuous-glow lamps. The complicated mathematics employed in the first and third papers makes possible a comparison of only individual experimental points with the

calculation results, and does not give a complete picture of the connection between parameters. The much more approximate calculation used in [119], based on the concepts of thermodynamic equilibrium, scattering of electrons by the ions, homogeneity of the discharge column over the tube cross section, and energy loss by recombination on the walls and by hydrogen-like recombination radiation, has made it possible to derive the fundamental experimentally-observed dependences of the discharge characteristics in tubular flash lamps on the parameters. In the case of insignificant reabsorption of radiation, such as prevails in lamps of 2—10 mm in diameter with electric gradient below 200—20 V/cm [88,125], calculations with the use of the formulas of Saha, Gvozdover, and Kramers [69, 81,181] has yielded the variations of ρ, T, and η (efficiency of the discharge as a radiation source) with the electric gradient and tube radius, as shown in Figs. 8 and 9. The thin lines of Fig. 8 are the plots of ρ calculated on the basis of the already mentioned assumptions, while the dashed lines are plots calculated with the aid of the same equations, but with two

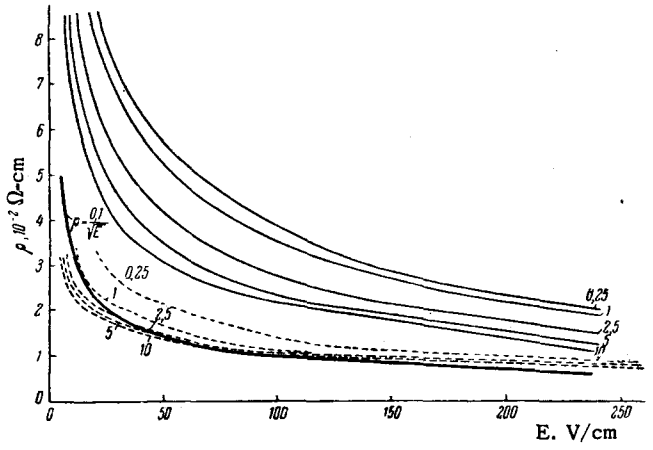

FIG. 8. Plots of $\rho = f(E)$, calculated for krypton lamps with internal tube radii 0.25, 1, 2.5, 5, and 10 mm. The solid lines correspond to approximate calculations, dashed lines – to formulas calculated with numerical coefficients corrected by means of a separate set of experimental quantities, thick line – plot of the empirical relation (5).

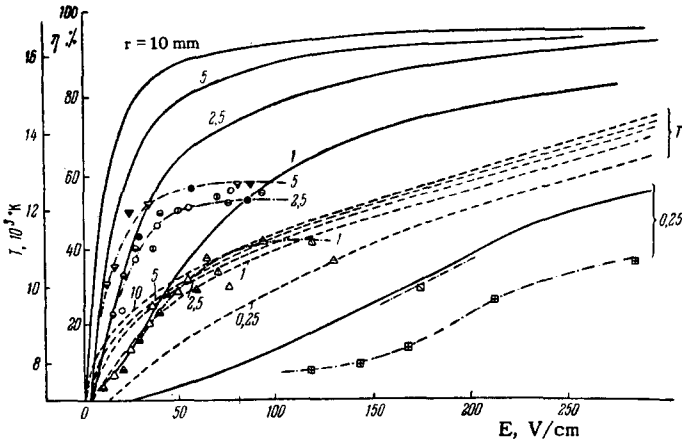

FIG. 9. Calculated plots of the dependence of the plasma temperature T on E (dashed) and on the discharge efficiency η (solid lines), obtained for corrected coefficients. Krypton, p = 100 mm Hg, l = 50 cm, r = 0.25, 1, 2.5, and 5 mm. Dash-dot line – averaged experimental plots of η, plotted on the basis of the following points: □ – r = 0.25 mm, Δ – 1 mm, ○ – 2.5 mm, ▽ – 5 mm (filled experimental points were obtained for C > 600 μF, half-filled points – 125 μF, unfilled – 80 μF, with vertical bar – 48 μF, horizontal bar – 14 μF, cross – 0.25 μF.[122,131]

numerical coefficients made more precise by means of a separate set of experimental values of all the parameters. Calculation yields also a correct estimate of the weak dependence of ρ on the type and pressure of the gas. Thus, the approximately unique dependence of ρ on E, obtained for almost all experimental conditions and expressed by formula (5), is also theoretically justified.

III. EXPANSION OF DISCHARGE CHANNEL

The expansion of the channel plays different roles for the two types of pulse discharge—with bounded and with unbounded channels. In the former the expansion usually terminates in an early phase of the process, followed by a rather prolonged discharge with constant column diameter and slowly varying characteristics, during the course of which the major fraction of the energy is dissipated in the gas gap. In the second the expansion of the channel continues for the entire time during which appreciable energy is dissipated in the gas gap. Consequently most investigations of channel expansions pertained to an unbounded discharge, whereas in the case of tubular lamps only a few investigations were devoted to this process.

3.1. Expansion of Channel in Tubular Flash Lamps

The clearest picture of the expansion of the channel in tubular lamps was obtained by Cloupeau [21,22] and by leComte and Edgerton [91], who used small supply capacitors, so that the duration of the discharge exceeded but slightly the time of its expansion. Cloupeau [21,22] photographed by means of a scanning mirror a section of the discharge channel, framed by a slot, while in [91] the end of the channel (visible at the bend of the tube) was photographed at different instants of time with the aid of a magnetooptical shutter with an effective exposure of about 1 microsecond. It was established in these investigations that the hottest portion of the gas, usually produced after the ignition of the discharge near the walls of the tubes along the igniting

electrode which is on the outside, expands rapidly until it fills amost the entire cross section of the tube. The rate of this expansion, measured in a xenon lamp with inside diameter 3.5 mm at a pressure 300 mm Hg and at an initial electric gradient ~200 V/cm ($E/p_0 \sim 0.67$ V/cm-mm Hg) is 600 m/sec. At other values of E/p_0 (the measurements were made in the range from 0.2 to 1 V/cm-mm Hg) it was found that the rate at which the channel cross section area increases is proportional to E/p_0, with a proportionality coefficient equal to 2.5 if the area is in square millimeters, the time in microseconds, and E/p_0 in V/cm-mm Hg. Under these conditions this corresponded to the following dependence of the speed of the expansion front dr/dt on the gradient

$$\frac{dr}{dt}\left[\frac{\text{mm}}{\mu\text{sec}}\right] \cong 0.9\frac{E}{p_0}\left[\frac{\text{V}}{\text{cm-mm Hg}}\right]. \qquad (7)$$

With decreasing atomic number of the gas in the lamp, the rate of expansion increases somewhat (by about 20 per cent on going from xenon to krypton or from krypton to argon). Some 5 microseconds after the ignition of the discharge, the front of the expanding channel almost reaches the opposite wall of the tube, and compresses against it the region of cold (non-glowing) gas with rather small cross section (~ 1 mm^2, about 10 per cent of the tube cross section), to a high pressure. Subsequently this region expands for a certain time (about 2.5 microseconds), pinching the hot channel so that its cross section decreases by about 20 per cent. After another time interval of the same length the hot channel again compresses the cold region, etc., until the oscillating between the hot and cold regions is gradually erased by the mixing of the gas. An analogous process of compression and subsequent expansion of the cold gas was observed also in the axial direction of the tube. The longitudinal compression and expansion waves propagate approximately at the same rates as the transverse ones, causing short-duration longitudinal inhomogeneities in the channel brightness; the instant when the brightness is increased occurs several microseconds after the instant of maximum increase in gas density. The duration of this process depends on the length of the tube and, naturally, exceeds greatly the duration of the transverse oscillations of the gas density.

3.2. Theory of Expansion of Unbounded Channel of a Pulsed Discharge

It is most convenient to systematize the extensive data accumulated in numerous experimental investigations devoted to the expansion of an unbounded channel,* by first presenting some notions concerning the theory of the expansion process, as developed in [182, 32,166,16,138]. In the first of these investigations, all of which were in general similar in method* and in the calculation results, a spherical problem was considered of an explosion produced by instantaneous release of energy in a point. The other papers deal with an explosion produced by energy released in a cylindrical channel. We present here a brief summary of the calculations of Drabkina, which are easiest to compare with the factual data, including the materials obtained by the experiments specially carried out for this purpose [1,2,31,63].

The calculation starts out from the assumption that the expansion of the channel is a purely hydrodynamic process of explosive type, and proceeds exclusively under the action of the energy released in a short time in a concentrated volume.

We use in the calculation a system of equations for the continuity, motion, and the hydrodynamic adiabat for cylindrical symmetry, and as the boundary conditions we use mathematical expressions that define the continuity of matter, motion, and energy on the boundary of the disturbed region (on the front of the shock wave):

$$\left.\begin{aligned} \frac{\partial\delta}{\partial t} + v\frac{\partial\delta}{\partial r} + \delta\frac{\partial v}{\partial r} + \frac{\delta v}{r} = 0, \\ \frac{\partial v}{\partial t} + v\frac{\partial v}{\partial r} + \frac{1}{\delta}\frac{\partial p}{\partial r} = 0, \\ \left(\frac{\partial}{\partial t} + v\frac{\partial}{\partial r}\right)\frac{p}{\delta^\gamma} = 0, \end{aligned}\right\} \qquad (8)$$

$$\frac{\delta_0}{\delta_f} = \frac{\gamma-1}{\gamma+1}, \quad v_f = \frac{2}{\gamma+1}D, \quad p_f = \frac{2\delta_0}{\gamma+1}D^2. \qquad (9)$$

δ —density, p —pressure, v —velocity of gas, r and t —cylindrical coordinate and the time, $D = dR/dt$ —velocity of the front of the shock wave of radius R, and γ —a constant which in the case of a perfect gas is equal to the ratio of the specific heat at constant pressure and volume; the subscripts "0" and "f" indicate the initial value of the given parameter or its value on the front of the shock wave.

It is known from hydrodynamics that the solution of this system of equations for a perfect gas and for an instantaneous explosion of rather high power (such that $p_f \gg p_0$), concentrated in an infinitesimally thin column of gas, is "self-similar," namely the distributions of δ/δ_0, p/p_f, and v/v_f are stationary with respect to the dimensionless coordinate $\xi = r/R$. The expression for R is obtained in this case from dimensionality considerations

$$R = \sqrt[4]{\frac{\alpha\mathcal{E}_0}{\delta_0}}\,t^{1/2}; \qquad (10)$$

here $\mathcal{E}_0$ —explosion energy per centimeter of length of the gas column, α —dimensionless constant which de-

*To make an understanding of the following material easier, we use the term "channel" for the entire region of gas disturbed by the discharge, and the term "discharge column" for the conducting part proper of the strongly ionized gas heated to high temperature.

*A general analytical method for the solution of similar hydrodynamic problems has been developed in the previously published papers by Sedov[167,168].

pends only on γ and can be calculated from the energy integral.

Assuming that for a real gas in the temperature range of interest to us (10,000—30,000°K) the equation of state has the approximate form

$$\varepsilon = A\delta^a T^b \qquad (11)$$

[ϵ —specific energy, T —temperature, A, a, and b — numerical coefficients calculated by trial such as to make expression (11) derivable from the equation $\epsilon = 3RT(1+x) + \epsilon_{diss} + 2x\epsilon_{ion}$, where ϵ_{diss} and ϵ_{ion} are the dissociation and ionization energies of 1 mole of gas and x is the degree of ionization calculated by Saha's formula (2)], we can reduce this equation to the form

$$p = (\gamma - 1)\varepsilon\delta. \qquad (12)$$

This equation agrees formally with the corresponding expression for a perfect gas, although γ is no longer the ratio of the specific heat, but merely an arbitrary quantity, connected with the coefficients (11) by means of the equation

$$\gamma = 1 - \frac{a}{b-1}; \qquad (13)$$

The numerical values of the coefficients for different gases are given in Table III.

Because of such a formal agreement, the adiabat equation for a real gas has the same form $p/\delta^\gamma = \text{const}$, as for a perfect gas, and the case of a real gas admits of a self-similar solution of the problem by using the value of γ from (13).

Plots of the corresponding pressure and density distributions for $\gamma = 1.22$ (air) are shown in Fig. 10. In the region $\xi = r/R \ll 1$ these distributions are approximately expressed by the following first terms of the rapidly-converging expansions of the corresponding functions:

$$\frac{\delta}{\delta_f} \cong \left(\frac{\gamma}{2}\right)^{\frac{2}{2-\gamma}} \xi^{\frac{2}{\gamma-1}} \left[1 + \frac{2}{\gamma+1}\xi^{\frac{2\gamma}{\gamma-1}}\right],$$
$$\frac{p}{p_f} \cong \frac{\gamma+1}{2\gamma}\left(\frac{\gamma}{2}\right)^{\frac{\gamma}{2-\gamma}} \left[1 + \frac{1}{\gamma+1}\xi^{\frac{2\gamma}{\gamma-1}}\right]. \qquad (14)$$

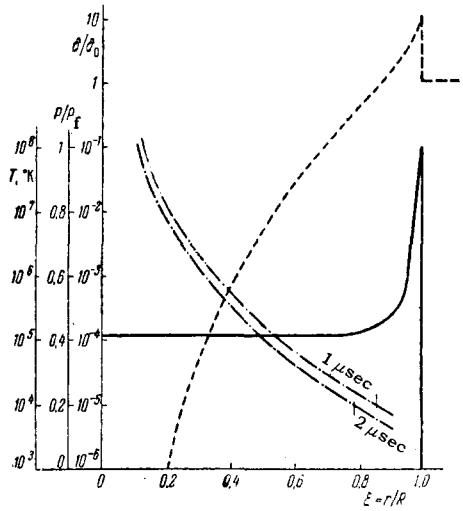

FIG. 10. Calculated radial distributions of the pressure (solid line), density (dashed), and temperature in the discharge channel at t = 1 and 2 microseconds (dash-dot). Air, atmospheric pressure, and energy $\mathcal{E} = 5$ J is released within the discharge column in an effective time interval t = 1 microsecond. The vertical bars on the temperature plots – arbitrary boundaries of the column at the corresponding instants of time and in units of r/R.[32]

It is possible to go over gradually from instantaneous release of energy in an infinitesimally narrow gas column to a gradual release by transforming formula (10). For this purpose we take into consideration the proportionality between p_f and the average pressure, which in turn is proportional to $\mathcal{E}(t)/R^2$ [$\mathcal{E}(t)$ —energy released by the instant of time t], and, using the last equation of (9), we obtain $\mathcal{E}(t)/R^2 = \text{const}\,(dR/dt)^2$, from which we get after extracting the square root and integrating a more exact expression for R in place of (10)

$$R = K\left[\int_0^t \mathcal{E}^{1/2}(t)\,dt\right]^{1/2} = \left(\frac{\alpha}{\delta_0}\right)^{1/4}\left[\int_0^t \mathcal{E}^{1/2}(t)\,dt\right]^{1/2}; \qquad (15)$$

we choose the constant K to make (15) go over into (10) if the energy is released instantaneously.

From (15) and the last equation of (9) we then get

Table III. Numerical values of the coefficients contained in formulas (9)—(20)

Gas	p_0, mm Hg	$\delta_0 \times 10^3$	a	A	a	b
Air	760	1.29	0.55	$6.9\cdot10^4$	$-1.22\cdot10^{-1}$	1.55
»	200	0.339	0.55	$6.9\cdot10^4$	$-1.22\cdot10^{-1}$	1.55
»	2300	3.87	0.55	$6.9\cdot10^4$	$-1.22\cdot10^{-1}$	1.55
Argon	760	1.78	0.332	1.35	$-1.25\cdot10^{-1}$	2.75
Hydrogen	760	0.0899	5.4	$4.33\cdot10^6$	$-9.3\cdot10^{-2}$	1.37

Gas	γ	K	L	M	N
Air	1.22	4.55	$1.9\cdot10^{-1}$	$1.25\cdot10^{-1}$	$3.76\cdot10^{-1}$
»	1.22	6.35	$2.92\cdot10^{-2}$	$1.25\cdot10^{-1}$	$3.76\cdot10^{-1}$
»	1.22	3.46	$1.33\cdot10^{-1}$	$1.25\cdot10^{-1}$	$3.76\cdot10^{-1}$
Argon	1.075	3.7	1.1	$4.3\cdot10^{-2}$	$4.6\cdot10^{-1}$
Hydrogen	1.25	8.85	$4.4\cdot10^{-1}$	$1.38\cdot10^{-1}$	$3.63\cdot10^{-1}$

$$D=\frac{dR}{dt}=\frac{K}{2}\mathscr{E}^{1/2}(t)\left[\int_0^t \mathscr{E}^{1/2}(t)\,dt\right]^{-1/2}, \tag{16}$$

$$p_f=\frac{(\alpha\delta_0)^{1/2}}{2(\gamma+1)}\mathscr{E}_0(t)\left[\int_0^t \mathscr{E}^{1/2}(t)\,dt\right]^{-1} \tag{17}$$

Transforming (11) and (12) into $T^b p\delta^{-(\alpha+1)/(\gamma-1)}A$ and inserting (14), (15), and (17) we can find the temperature distribution inside the channel

$$T^b=\frac{1}{4A\gamma}\left(\frac{\gamma}{2}\right)^{\frac{\gamma-2a-2}{2-\gamma}}(\gamma+1)^{-a+1}(\gamma-1)^a\alpha^{\frac{\gamma+a}{2\gamma-1}}\delta^{\frac{a-\gamma-2a\gamma}{2(\gamma-1)}}r^{-\frac{2(a+1)}{\gamma-1}}$$
$$\times\mathscr{E}(t)\left[\int_0^t \mathscr{E}^{1/2}(t)\,dt\right]^{\frac{2+a-\gamma}{\gamma-1}}. \tag{18}$$

Figure 10 shows the corresponding plots of the temperature distribution for typical discharge conditions at a time t = 1 microsecond (directly after the energy release stops) and another microsecond later.

If we assume that the boundary of the highly ionized conducting column of the discharge is characterized by the fact that the temperature inside the column exceeds a definite minimum value T_{lim}, say 10,000°K (the specific choice of the value of T_{lim} is immaterial, in view of the steepness of the T vs. r curve), then, by substituting this value into (18), we can find the corresponding value of r_c —the radius of the conducting column. The time derivative of r_c is equal to the rate of expansion of this column. From (18) we obtain for these quantities the following expressions:

$$r_c(t)=L\mathscr{E}^M(t)\left[\int_0^t \mathscr{E}^{1/2}(t)\,dt\right]^N, \tag{19}$$

$$\frac{dr_c(t)}{dt}=L\mathscr{E}^{M-1}(t)\left[\int_0^t \mathscr{E}^{1/2}(t)\,dt\right]^N$$
$$\times\left\{M\frac{d\mathscr{E}(t)}{dt}+N\mathscr{E}^{1/2}(t)\left[\int_0^t \mathscr{E}^{1/2}(t)\,dt\right]^{-1}\right\}. \tag{20}$$

Here M and N are coefficients that can be expressed in terms of γ and a (they are independent of the gas density), while L can be expressed in terms of γ, a, b, A, α, δ_0, and T_{lim}. The values of all the coefficients (in CGS units) are given for some gases in Table III, which is taken from [32].

Finally, if we take into account the fact that in the later phase of channel expansion the condition $p_f \gg p_0$ is no longer satisfied, we must take in place of the first and last equations in (9)

$$\frac{\delta_f}{\delta_0}=\frac{(\gamma+1)p_f-(\gamma-1)p_0}{(\gamma-1)p_f+(\gamma+1)p_0}, \qquad D^2=\frac{(\gamma+1)p_f-(\gamma-1)p_0}{2\delta_0}. \tag{21}$$

From (21), which take into account the fact that during the last phase of the expansion one can no longer neglect the external pressure of the unperturbed gas, it follows that in this case a ledge should gradually appear on the plots showing the decrease in density and pressure away from the front of the shock wave toward the discharge axis, beyond which a high density gradient should be observed with a sign opposite that of the negative $d\delta/dr$ on the leading front.* In other words, the region of gas with increased density should also be separated by a jump δ from the internal "hot" region (the column). The radius of the zone of this jump, which is called the "sheath" of the channel, is larger than the radius of the highly ionized region of the column as defined by (19).

Thus, the notion that the expansion of the channel of a powerful pulsed discharge is a purely hydrodynamic process leads to the following picture of the development of a discharge with unbounded channel:

a) The fastest to propagate should be the zone of the jump in the density and pressure (from high values to values corresponding to the unperturbed medium), which is the outermost boundary of the channel, namely the front of the shock wave. The region of strongly heated highly ionized plasma, which is the conducting gas column proper, practically coincides at the start of the discharge with the space inside the front of the shock wave, after which it gradually unravels from the front and expands at a slower rate. With decreasing pressure on the front, there should appear between the column and the shock-wave front a zone of inverse density jump ("sheath"), which expands at a velocity intermediate between the rates of expansion of the front and the column.

b) Inside the conducting column the gas density should be several orders of magnitude lower than δ_0, and should decrease even more on going from the periphery to the axis of the channel. Because of this, a zone with anomalous plasma resistivity may be formed on the axis of the column.

c) The expansion of each of the channel zones should proceed with gradually decreasing speed, the initial value of which (which is common to all zones) increases weakly with increasing α (which characterizes the type of gas), with decreasing initial gas density, and with increasing instantaneous power and total energy dissipated in the channel.

By using the formulas of the hydrodynamic theory and the data on the electric characteristics of the column (Chapter II) we can obtain an approximate estimate of the order of magnitude of the initial rate of channel expansion, and also calculate tentatively the effect of the individual parameters of the gas gap and the supply circuit on this initial velocity.† We simul-

*It was erroneously indicated in [32] that the density should be approximately constant between the front of the shock wave and the zone of high and positive $d\delta/dr$. Since T cannot decrease in the direction from the front to the discharge axis, the drop in the gas pressure in this direction (see Fig. 10) should correspond qualitatively to a similar drop in its density[31].

†In recent papers the hydrodynamic theory of channel expansion is developed both in application to problems with different types of symmetry (including the problem of a "plane" explosion in a T-shaped discharge tube [70a, 79, 138]), and as applied to a simultaneous

taneously calculate the voltage U_i on the discharge, immediately after termination of the vigorous growth of the current density, something that could not be done in Chapter II for lack of an idea concerning the mechanism of channel expansion.

From (16) we can obtain the instantaneous release of all energy, assuming that

$$D=\frac{1}{2}\left(\frac{\alpha\mathcal{E}_0}{\delta_0}\right)^{1/4}t^{-1/2}. \quad (22)$$

Considering that the discharge voltage U_i at the first instant after the termination of the vigorous growth of the current density is equal to the difference between the capacitor voltage U_0 and the drop across the inductance, $L\,dI/dt$, and assuming in accordance with (5) that

$$I=10\pi\left(\frac{U_i}{l}\right)^{3/2}r_c^2$$

and

$$\frac{dI}{dt}=62.8\left(\frac{U_i}{l}\right)^{3/2}r_cD,$$

we obtain

$$\frac{U_i}{l}=\frac{U_0}{l}-62.8r_c\frac{L}{l}D\left(\frac{U_i}{l}\right)^{3/2}. \quad (23)$$

In formula (22) we can substitute the approximate expression for $\mathcal{E}_0$ (in ergs):

$$\mathcal{E}_0=10^7\frac{U_i}{l}It=10^8\pi r_c^2t\,\frac{U_i^{5/2}}{l^{5/2}}$$

(neglecting radiation, which plays a negligible role at the start of the expansion when the diameter is small [63]), from which we get a second equation relating U_i and D:

$$D=\frac{1}{2}\sqrt{\frac{10^8\pi\alpha}{\delta_0 t}}\,r_c^{1/2}\,\frac{U_i^{5/8}}{l^{5/8}}. \quad (24)$$

Substituting into (23) and (24) the numerical values of the constants from Table III, assuming realistic values for the effective time $t = 5 \times 10^{-8}$ sec and for the initial radius of the column $r_c = 10^{-2}$ cm, we can obtain from this system of equations D and U_i/l for different specified values of U_0/l and L/l. The corresponding plots are shown in Figs. 11a and b. Instead of using the system (23) and (24), which is not convenient for practical work, we can derive from Fig. 11 empirical formulas, which can serve for a generalization of the experimental data*:

$$D=0.166\left(\frac{\alpha}{\delta_0}\right)^{0.25}\left(\frac{L}{l}\right)^{-0.25}\left(\frac{U_0}{l}\right)^{0.32}, \quad (25)$$

$$\frac{U_i}{l}=0.34\left(\frac{L}{l}\right)^{-0.42}\left(\frac{U_0}{l}\right)^{0.5}; \quad (26)$$

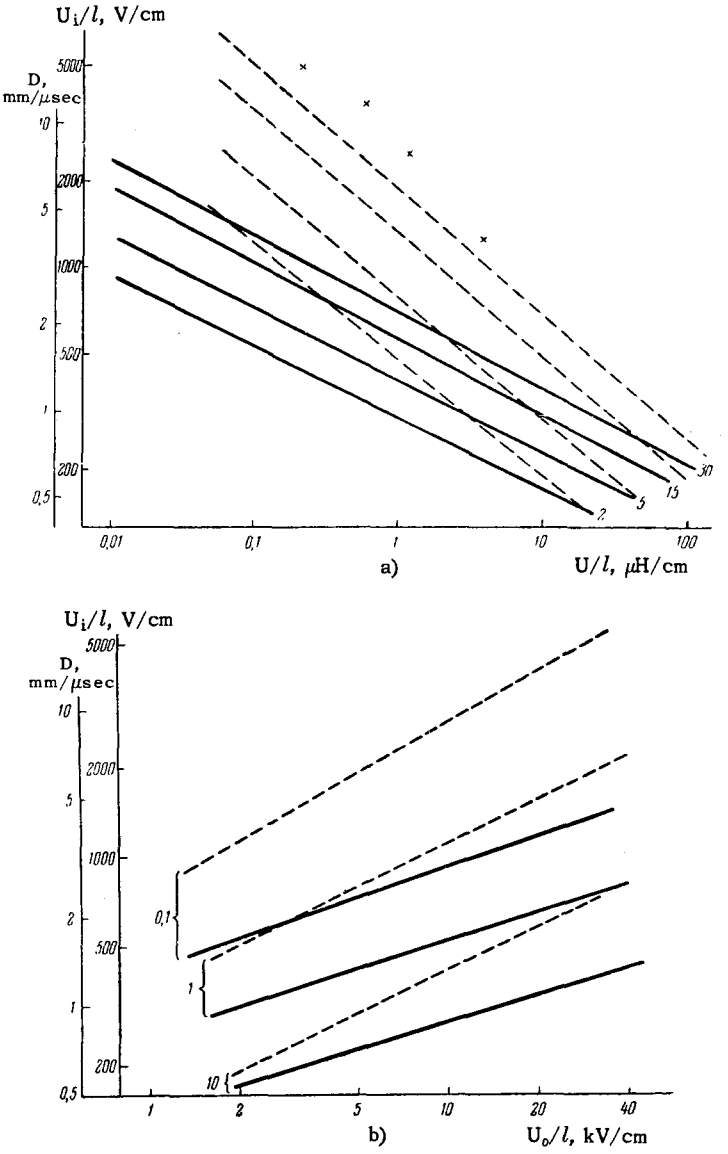

FIG. 11. Theoretical plots of the dependence of the electric gradient in the discharge at the instant of termination of the vigorous growth of current density, U_i/l (dashed curve), and of the initial velocity D of the channel expansion (solid lines), on the inductance of the discharge circuit (a) and the voltage on the supply capacitor (b). Air, atmospheric pressure. In Fig. (a) the numbers designate the values of U_0/l corresponding to each line, in kV/cm, and in Fig. (b) – the values of L/l in μH/cm. The crosses on Fig. (a) denote the experimental values of U_i/l for air at $U_0 = 6$ kV and $l = 4$ mm.[3]

solution of the hydrodynamic problem and the problem of calculating the energy released in the channel[16]. In the present review, which is aimed at generalizing the principal experimental data, it is not advisable to go into details of the complicated mathematics of these papers. Their principal quantitative results generally agree with experiment to the same degree as the results of the simplified theory (including the estimate given above for the energy release), and the detailed assumptions and conclusions are still in the discussion stage and need experimental verification.

*No detailed experimental investigation was made of the dependence of U_i on the discharge parameters. However, judging from a comparison of (26) with individual measurements (see, for example, the experimental points on Fig. 11a for a discharge in air at atmospheric pressure, $U_0 = 6$ kV, gap length 4 mm, $U_0/l = 15$ kV/cm, taken from [3]), it agrees satisfactorily with experiment both in the character of the dependences and in order of magnitude of U_i. A more accurate agreement would be obtained if the coefficient 0.34 were replaced by 0.7. A comparison of (25) with experiment is given in the next section.

D is in mm/μsec, L is in μH, U_0 and U_i are in kV, and l is in cm.

In order to understand more readily which inaccuracies in the initial premises can cause the individual discrepancies between theory and experiment, let us list the processes that are not taken into consideration by these premises.

a) Dissipation of energy in different layers of the highly ionized column depends on the conductivities of these layers. This can influence the distribution of the temperature and of the gas density inside the column.

b) A similar influence can, generally speaking be exerted by the skin effect and by magnetic pressure. It is shown in [16] that in the range of discharge parameters considered here this influence is small. In fact, the depth d of penetration of the field during the time t can be estimated from the formula

$$d^2 \cong \frac{c^2 t}{2\pi} \frac{\varrho}{9 \cdot 10^{11}}.$$

Assuming $t \cong 1$ μsec, taking the corresponding column radius r_c to be ~ 0.1 cm, and estimating ρ from formula (5), we obtain $r_c/d \cong 0.02\, E^{1/4}$, that is, at least one order of magnitude less than unity for E up to 1000 V/cm. We can thus assume that the field should be practically constant over the cross section. In exactly the same manner, the ratio of the magnetic pressure $A^2/8\pi$ to the gas-kinetic pressure can be estimated at $(r_c/d)^2$ [16], so that the magnetic forces can be neglected. At the same time, the estimates made show that at appreciably smaller initial gas densities, and also at rather high electric gradients and large discharge energies, at which the radius of the column can be one order of magnitude larger than that assumed, the skin effect and magnetic pressure should play an appreciable role. As is known, this actually occurs in pulsed discharges such as lightning[144,145], and also in discharges used in laboratories to obtain superhigh temperatures [80]. The particular instability of the column of short discharges in hydrogen [49] is possibly due to the role of magnetic forces, which are appreciable for such discharges. At the same time one can assume on the whole that the absence of significant magnetic forces is a distinguishing feature of the aggregate of powerful pulse discharges, considered in the present review.

c) The calculations do not reflect any form of radial energy transfer other than hydrodynamic expansion. The energy supplied to the discharge and lost by radiation can be formally taken into account in the derived equations by subtracting the corresponding fraction of energy from the value of $\mathcal{E}(t)$ (such a correction for the radiation from a column, equal to the radiation of a black body, is made in [63], while a correction for hydrogen-like radiation is made in [16]). Other forms of transport are more difficult to estimate. Glaser [67] suggests, for example, that the channel may be capable of expanding only by radial diffusion of the electrons and by radiation. On the other hand, in the paper by Abramson et al [12], which served as the basis for the development of the hydrodynamic theory, it is denied that a corresponding role is played by diffusion of electrons and ions, photoionization of the gas surrounding the channel (diffusion of radiation), and heat transfer to the surrounding volume by convection and heat conduction, since these processes cannot explain the supersonic velocity at which the channel expands, and for which a pressure jump on the order of tens of atmospheres is necessary. It is shown in [16] that the transport of heat in the channel at relatively low temperatures (low energy concentrations as a result of the large inductance or small supply voltage) can be produced by heat conduction, while at high temperatures it can be caused by radiation.

The picture of radial distribution of density and temperature, obtained from purely hydrodynamic theory and showing these quantities to have very high gradients within the column (Fig. 10), evidences that other forms of energy transfer should play a principal role near the axis and reduce these gradients.

3.3. Experimental Data on the Expansion of an Unbounded Channel

The expansion of the channel of an unbounded discharge was investigated by a whole series of methods, namely:

a) Photographic scanning of the picture of the transverse section of the channel, by means of a slot moving in front of the channel [54,64,65,71,80,84,117,173,216].

b) Similar scanning with simultaneous additional flashing of the space surrounding the channel with the aid of a second spark, using the Toepler shadow method [2,63,116].

c) Sweeping on the screen of an electron-optical converter the image of a narrow slot located ahead of the channel and perpendicular to its axis with simultaneous illumination of the space surrounding the channel by the shadow method, and using spectrum-selecting filters placed between the slot and the electron optical converter so that the blue and infrared radiation of the channel can be observed [197].

d) Super-high-speed motion picture photography of the discharge channel with the aid of an electron-optical shutter [49], a Kerr shutter [80], or a motion picture camera [131,196].

e) High-speed interferometry of the gas density in the channel and in the region surrounding it, by placing the investigated channel in one arm of an interferometer and illuminating it with a synchronized auxiliary discharge having a very short flash duration [31,116].

f) Observation of the distribution of the spots produced on the electrodes by pulsed discharges of different duration [170,177-179].

All the obtained experimental data confirm qualitatively and quantitatively the correctness of the picture of channel-boundary displacement, which follows from the hydrodynamic theory of the expansion process and from data on the electrical characteristics. At the same time, some experimental data concerning the physical characteristics inside the highly ionized plasma column do not confirm the existence of tremendous pressure and temperature gradients in this column. This means that the characteristics inside the column cannot be calculated without an account of processes which were not taken into consideration by the purely hydrodynamic theory.

To justify these conclusions, let us present a brief summary of the experimental material.

3.3.1. Expansion of the shock-wave front and of the sheath. Figure 12 shows samples of Toepler sweep photographs and interference photographs which show the expanding boundaries of the front of the shock wave,

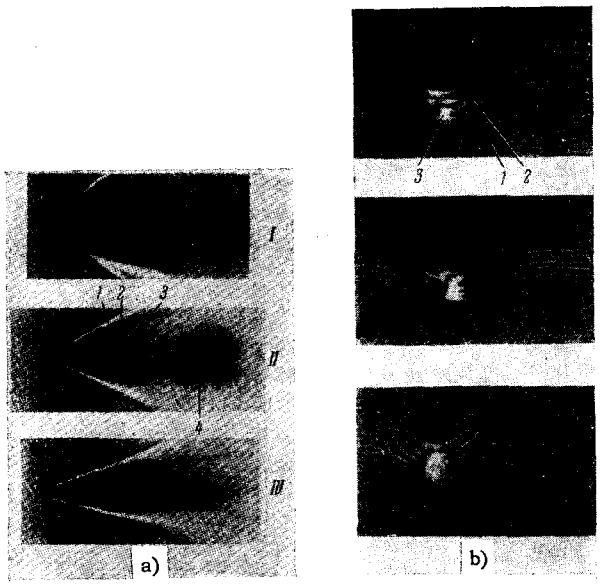

FIG. 12. Samples of (a) sweep photograph[63] and (b) interference pattern[31] obtained by the Toepler method. 1 – Front of shock wave; 2 – sheath; 3 – discharge column; 4 – secondary shock wave. Air, C = 0.25 μF. In Fig. a) U_0 = 15 kV, I – L = 2 μH, II – L = 12 μH, III – L = 64 μH. In Fig. b) U_0 = 10 kV, L = 2 μH, R_b = 6 Ω (the pictures were taken along the channel axis 3, 8, and 15 microseconds after the start of the discharge).

sheath, and conducting column. Similar photographs have enabled Mandel'shtam, Dolgov, Gegechkori, Vanyukov, and others [2,31,63,116,196,197,216] to note the following qualitative features in the expansion of the shock wave and the sheath, which agree with hydrodynamic theory and at the same time supplement its conclusions:

a) The sheath is not a surface of hydrodynamic discontinuity, since its speed can be both higher and lower than that of sound.

b) The sheath breaks down after several dozen microseconds following the start of the discharge, because by that time the pressure of the gas on the axis, which is approximately half the pressure on the front, becomes lower than atmospheric, and gas begins to flow toward the axis of the channel.

c) In the case of an oscillatory discharge, secondary shock waves are observed, due to the repeated release of energy in the column during each half cycle of the current. These waves appear to start on the sheath, since they are invisible inside the sheath as a result of the low gas density and the high velocity of the shock waves.

d) Inside the sheath there is a relatively cold zone, with low gas ionization, and a strongly heated highly ionized zone (the discharge column), the expansion of which slows down sharply at the instant of the first current maximum (apparently, after the shock wave breaks away from the channel, it continues to receive energy from the channel in the form of small perturbations, the speed of which exceeds the speed of the shock-wave front). The less heated zone has a sharp outer boundary, which coincides with the sheath. It emits principally the infrared arc lines and behaves like a pure surface emitter with respect to these lines; its brightness is constant over the entire cross section and does not change with current oscillations. Its expansion continues for several cycles of the current oscillations. The boundary between the less heated and high-temperature zones is blurred, owing either to the lower density of the current on the edges, or to the different depth of the glowing layer. The hot zone emits principally a short-wave continuous spectrum, the density of which noticeably increases at the instants of the current maxima and in the central part of the channel. Its expansion terminates after one or two current oscillations.

e) Extinction and increase in brightness of individual regions of the glowing column are observed at local compressions in these regions, due, for example, to focusing of the waves reflected from the walls of the discharge bulb, to the superposition of the shock wave traveling from the auxiliary discharge, or to the action of magnetic forces after the decrease in the gas density.

Measurements of the velocity of the shock-wave front under different conditions make it possible to make a quantitative comparison of the deductions of hydrodynamic theory with experiment. Figure 13 shows plots of the time variation of the velocity of the shock wave in air at atmospheric pressure for different discharge conditions, while Fig. 14 shows similar plots for different gases, and also for air at different pressures. The dashed curves on Fig. 14 are some of the corresponding plots calculated by Gegechkori[63] by means of the formulas of Sec. 3.2, using values of the electric power given in [1]. Figure 15 summarizes results of various measurements of the initial rate of discharge-column expansion, coinciding with

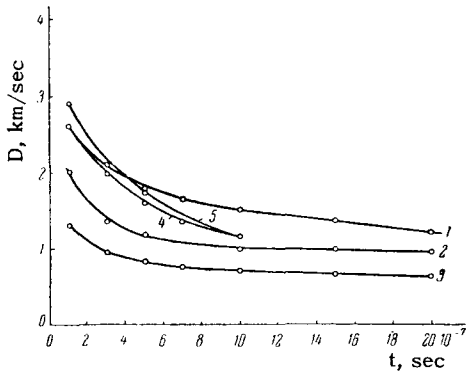

FIG. 13. Dependence of the time variation of V on the supply parameters[63]. Air, atmospheric pressure. 1 – L = 2 μH; 2 – L = 12 μH; 3 – L = 64 μH (for all three curves C = 0.25 μF and U_0 = 15 kV); 4 – U_0 = 15 kV; 5 – U_0 = 20 kV (for both curves L = 2 μH, C = 0.01 μF).

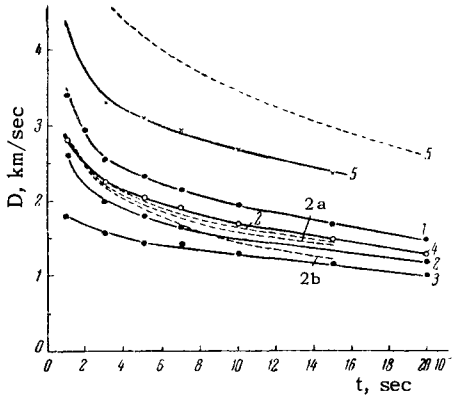

FIG. 14. Dependence of the time variation of D on the type and pressure of gas[63]. Solid lines – experimental data; dashed – calculated curves. L = 2 μH, C = 0.25 μF, U_0 = 15 kV; 1 – p = 200; 2 – p = 760; 3 – p = 2300 mm Hg (all three curves for air); 4 – argon; 5 – hydrogen (both curves p = 760 mm Hg). In calculating the course of curves 2a and 2b, the value of $\mathcal{E}$(t) was set equal to the electric energy fed to the discharge, minus the energy radiated by an absolutely black body having the same dimensions as the discharge column and having temperatures 15,000 and 20,000° K.

the initial velocity D of the shock-wave front. These data were obtained by the various methods listed above under various conditions, as listed in Table IV. They are summarized in a single plot on the basis of relationship (25), derived in Sec. 3.2, in which the inductance referred to a gap of length l = 1 cm has been taken, for the sake of clarity, to be the independent argument. The dotted line in the same figure is a plot of Eq. (25), and the solid line is a plot of an analogous relation with a different numerical coefficient (0.224 instead of 0.166), which can be regarded as a tentative averaging of the experimental data.

In spite of the large scatter of the points, which is natural in view of the differences in the measurement procedures, the inaccuracy in the calculation of the coefficient, and the approximate derivation of formula (25), Fig. 15 does permit us to assume that the theoretical dependence of D on various parameters is in satisfactory qualitative and quantitative agreement with the extensive experimental material; this becomes particularly convincing if we consider the location of the experimental points obtained by one and the same worker for one gas.

It follows from Figs. 13 and 14 that:

a) In accord with theory, a decrease of the supply capacitor does not influence the initial rate of expansion and is manifest only in a faster decrease of D with time (Fig. 13, curves 1 and 4);

b) The overall course of the experimental and theoretical curves is sufficiently close, particularly if radiation is taken into account, to make it possible to speak of satisfactory agreement between the approximate theoretical formulas and experiment.

Another way of qualitatively verifying the theoretical calculation of D was given by Dolgov and Mandel'shtam[31]. They measured, at different instants of time, the shifts in the interference fringes (Fig. 12b) of an interferometer which had the spark gap in one of its arms. The shift of the fringes, with an account

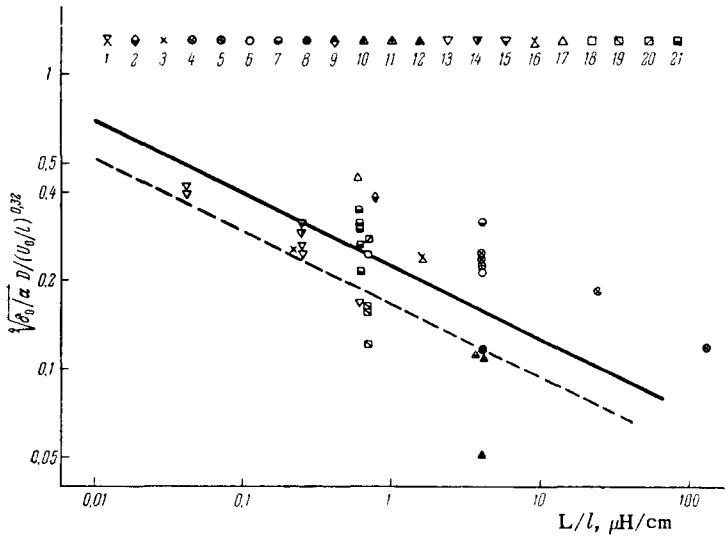

FIG. 15. Summary plot of the dependence of the initial rate of channel expansion on the kind and density of the gas, the length of the channel, the supply voltage, and the inductance of the supply circuit. The symbols for the points are listed in Table IV. Dashed line – calculated plot, corresponding to formula (25); solid line – tentatively averaged experimental plot (the numbers of the symbols correspond to those indicated in Table IV).

Table IV. Conditions under which different authors measured the initial velocity D_{in} of column expansion and the maximum column radius r_{max}

Designations used in Figs. 15 and 17*	Literature	Measurement method	Gas	p_0, atm	$\delta \times 10^3$, g/cm	l, mm	L, μH	U_0, kV	C, μF	$CU_0^2/2$, J
1	[7]		Air	1	1.3	8.4	0,01	20	0.005	1
2	[49]	Cinematography, electron optical converter	Ar	4.4	7.8	2	0.15	6	0.57	10.2
3	[54]**	Photosweep	Air	1	1.3	80—90	1.8—90	to 200	5.5	to 100000
4	[63]	Photosweep with shadow photography	Ditto	1	1.3	5	2—64	15—20	0.0035—0.25	0.4—28
5	[63]	Ditto	» »	0.26	0.35	5	2	15	0.25	28
6	[63]	» »	» »	3	3.9	5	2	15	0.25	28
7	[63]	» »	Ar	1	1.78	5	2	15	0.25	28
8	[63]	» »	H_2	1	0.09	5	2	15	0.25	28
9	[65]	Photosweep	Ar	11—17	19.5—30	7—11.2	0.36	10—14	0.1—0.2	5—20
10	[84]	Ditto	Air	1	1.3	11	3.6	10—35	0.06	3—40
11	[84]	» »	»	0.33	0.43	11	3.6	11	0.06	3.6
12	[84]	» »	H_2	1	0.09	11	3.6	17	0.06	8.7
13	[131]	Screen motion picture camera	$Xe+H_2$	3	15	5	0.02—0.3	5—7	0.005—0.1	0.05—2.5
14	[131]	Ditto	$Kr+H_2$	3	10	5	0.12	7	0.1	2.5
15	[131]	» »	$Ar+H_2$	3	4	5	0.12	7	0.1	2.5
16	[197]	Sweep, electron optical converter	Air	1	1.3	2.3	0.37	14	0.1	10
17	[197]	Ditto	Xe	4	23	6	0.35	24	0.1	29
18	[189, 217]	Photosweep	Kr	2	8	10	0.65	8	4	128
19	[189, 217]	Ditto	Kr	4	16	10	0.65	4—8	0.1	0,8—3.2
20	[189, 217]	» »	Kr	6	24	10	0.65	8	4	128
21	[216]	» »	Ar	1—4.8	1.78—8.5	10	0.6	2—7	1.1	2.2—13.6

*For the symbols corresponding to these numbers see Fig. 15.

**The supply parameters are not indicated in [54] and are estimated from data on the maximum current and the oscillation period, and also from the flash energy for the point: 9700 J, D_{in} = 2.4 km/sec.

Table V. Values of D at different instants of time after the start of the discharge in air (atmospheric pressure, U_0 = 15 kV, C = 0.25 μF, L = 2μH), obtained by different methods

t, μsec	D, km/sec				
	1	1.7	2.9	5.8	9.8
Direct measurement[63]	1.5	1.29	0.9	0.57	0.5
Measurements of δ_f[31]	1.75	1.28	0.88	0.57	0.49
Measurements of $\mathscr{E}(t)$[1]	1.65	1.4	—	—	—

of the depth of the corresponding layer of the channel, made it possible to determine the change in the refractive index, and consequently the density of the given layer; the measurements were carried out in the less heated zone near the front, for which one can neglect ionization and dissociation and use the ordinary connection between the refractive index and the gas density. The values of δ_f obtained from experiment (see, for example, Fig. 16) could be recalculated with the aid of formula (21) into the corresponding values of p_f and D. Thus, for example, the highest value of δ_f which could be obtained in accordance with the accu-

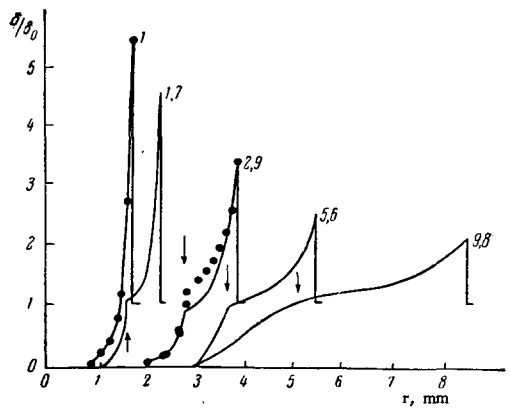

FIG. 16. Typical experimental (continuous lines) and calculated (dots) plots of the radial distribution of air density at different instants after the start of the discharge (time in microseconds). U_0 = 10 kV, C = 0.25 μF, L = 2 μH, p_0 = 760 mm Hg[31]. The arrows show the positions of the "sheath."

racy of the given method for t < 1 sec was $8\delta_0$; the theoretical value of δ_f for air when $p_f \gg p_0$ is $10.1\,\delta_0$. The corresponding values of the pressure and velocity of the front are p_f = 38 atm and D = 1.8 km/sec. The results of such a calculation of the values of D, based on the data of interferometric measurements at dif-

ferent instants of time, are listed in Table V, with direct measurements of D with the aid of mirror scanning [63] and with values of D calculated by formula (16) on the basis of measurements of the electric power of the discharge [1] (without account of radiation).

This table also demonstrates the satisfactory agreement between the approximate theory and experiment.

Finally, data on the radial distribution of the gas density at different instants of time, similar to those shown in Fig. 16, can be compared with the corresponding theoretical data, affording at the same time a qualitative check on the theory of channel expansion. The results of the theoretical calculation of the variation of δ at the instant $t = 1$ μsec [first formula of (14)] and at the instant $t = 2.9$ μsec [second formula of (14); it is assumed that the usual equation of state $p = R\delta T$ holds true in the less heated zone and that the temperature is constant in this zone] are designated by the points on Fig. 16. We see that this check also confirms satisfactorily the hydrodynamic theory.

3.3.2. Expansion of the discharge column. The boundary of the high-temperature zone of the channel —the discharge column after it becomes separated from the front of the shock wave, has a blurred character, and consequently data obtained by different workers concerning the later stages of the expansion of the column differ appreciably, since they depend strongly on the chosen boundary criterion, namely a definite value of photographic density.

The column-expansion process is best characterized by means of two parameters, the initial rate of expansion and the column radius r_{max} after its maximum increase.* The initial rate of column expansion practically coincides with the initial velocity of the shock wave, data on which were given in Sec. 3.3.1. Summary data on the effect of discharge conditions on r_{max}, gathered from work done by many authors (see Table IV), are presented in Fig. 17 in the form of plots of r_{max} vs. the energy of the supply circuit.

As can be seen from Fig. 17, in spite of the difference between the experimental procedures and the criteria of the column boundary, the points cluster close enough about the plot to disclose a general dependence of r_{max} on the parameters. The strongest influence is exerted on r_{max} by the energy $CU_0^2/2$. For air at atmospheric pressure one can assume the empirical formula

$$r_{max} = 0.5\left(\frac{CU_0^2}{2}\right)^{0.4}, \qquad (27)$$

where r is in mm, C in μF, and U in kV.

*Glaser[67] proposes to characterize it by means of other parameters, namely r_{max} and the period of the current oscillations in the discharge. The latter, however, is too indirectly connected with the physical phenomena in the discharge. Although it is connected more or less uniquely with D_{in} and r_{max}, it is not convenient to use this parameter for a practical determination of the course of the increase of r_c with time.

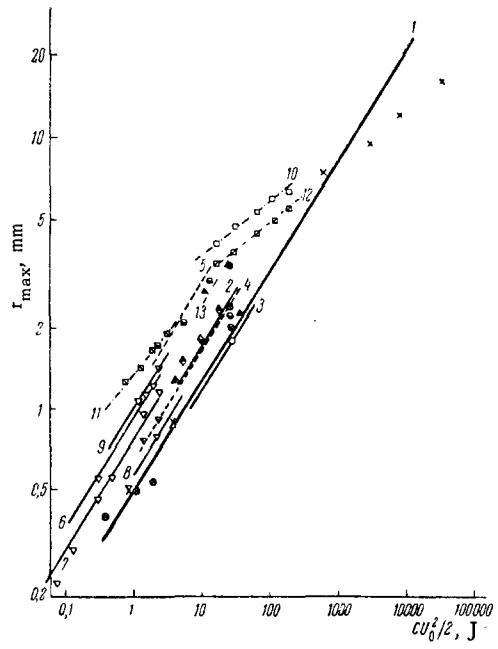

FIG. 17. Summary plot of the dependence of the maximum discharge-column radius on different parameters of the discharge gap and of the supply circuit. 1, 2, 3 – air, pressure 1, 0.3, and 3 atm, respectively; 4, 5 – argon, pressure 1 and 3–11 atm; 6, 7, 8 – xenon with hydrogen added, pressure 3 atm, inductance 0.02, 0.12, and 0.3 μH, respectively; 9 – krypton with hydrogen added, 3 atm, 0.12 μH; 10, 11, 12 – krypton at 2, 4, and 6 atm, 0.6 μH; 13 – hydrogen, 1 atm (for symbols see Fig. 15 and Table IV).

A decrease in the gas pressure and in the inductance of the discharge circuit by almost one order of magnitude increases r_{max} only by 15—30 per cent. The capacity and the voltage taken separately (with $CU_0^2/2$ constant) hardly influence the value of r_{max}. It is in general difficult to speak of an influence of the kind of gas, owing to the difference in the character of the glow and transparency of the column, particularly during the later stage of channel expansion. Thus, for example, in the case of a discharge in argon the column becomes so blurred by the end of the expansion, that in [131] lower estimates were obtained for its diameter, the other parameters remaining the same, than for the diameter of the discharge column in krypton or xenon, which at first expands much more slowly.* The discharge column in hydrogen is so unstable, judging from the instantaneous photographs obtained by Fischer [49] with the aid of an electron optical converter, that already 1—1.5 μsec after the start of the discharge one cannot speak at all of any definite diameter of the column; as indicated at the end of Sec. 3.2, this may be attributed to the action of magnetic forces.

The position of the plots for different gases on Fig. 17 shows nevertheless that the difference between the corresponding values of r_{max} is not too large (it

*An analogous explanation can probably be given for the essential difference between plots 10–12 and the remaining data on Fig. 17.

does not exceed ~ 60 per cent with other conditions equal). Formula (27) can thus be extended to use for estimates under all possible discharge conditions encountered in practice. If we replace the coefficient 0.5 in this formula by 0.65, then the deviations of the actual values of r_{max} from those calculated by this formula will not exceed as a rule 20—25 per cent.

The available experimental materials enable us to draw certain conclusions not only on the column boundaries, but also on its internal characteristics. The processing of interference patterns similar to that shown in Fig. 12b has enabled Dolgov and Mandel'shtam [31] to estimate roughly the mean gas density in the internal part of the column (by subtracting from the overall volume of the perturbed gas the amount of gas concentrated in the relatively cold high-density zone, and also the corresponding concentration of the electrons [from the negative value of $(n-1)$, where n is the measured refractive index of this zone of the column*]. The result yielded practically equal concentrations of atoms and electrons ($\sim 10^{17}$ cm^{-3}), which were approximately constant over the entire cross section of the hot portion of the column. Confirmation of such a conclusion would denote that the rather high density and temperature gradients, which by hydrodynamic theory should increase on approaching the axis (see Fig. 10), are actually missing from the inside of the column or have a considerably smaller magnitude than on the boundary of the column. The equalization of the temperature and density would be naturally tied in in this case with processes of the diffusion type.

However, it is difficult to tie in the conclusion of [31] with the results of Somerville et al [177,179], devoted to a study of the space-time distribution of spots on a pulse-discharge anode (air, pressure close to atmospheric, l several millimeters). To obtain reproducible results, the anode was covered in these experiments by a homogeneous insulating film several times 10 millimicrons thick. During the course of the discharge, electrons accumulate on this film until local breakdowns of the dielectric take place, after which the near-anode potential drop "focuses" the new arriving electrons into the "holes", causing the latter to expand gradually and molten spots to form on the metal. The position and dimensions of the spots for different pulse-discharge durations make it possible to estimate the electric conductivity of the adjacent part of the column. By using current pulses of different strength, with different rise times, and also using doubled current pulses following each other after an adjustable time interval, the authors of these papers have established that first to form during the period when the discharge channel expands are "holes" near the axis, which then "escape" as it were as a result of the decreased conductivity of the plasma in this region, and new "holes" are formed closer to the column periphery. The rate of radial displacement of the belt of "acting holes" agrees during the first 0.1 μsec with the calculated values of D, obtained from formulas (16) and (22) of the hydrodynamic theory, which, in the authors' opinion, confirms the idea that a correspondence exists between the instantaneous position of these "holes" and the conducting zone of the column. The existence of a "hollow" zone near the column axis would indicate that the distribution of the gas density and of the temperature inside the column have appreciable gradients.

At the present time the question of the actual distribution of the density and temperature inside the column, and consequently of the role of the physical processes taking place inside the column and not accounted for by hydrodynamic theory, still remains open.

*Such a method of estimating the average gas density in the hot zone nevertheless raises serious doubts concerning the correctness of even the order of magnitude of the result obtained. In fact, in order to obtain the value $\delta_{av} = 5 \times 10^{-6}$ g/cm^3, cited by the authors, one would have to carry out a graphic integration of the gas mass in the cold zone with an accuracy to 0.1 per cent.

IV. RADIATION CHARACTERISTICS

4.1. Radiation Intensity

The pattern of the dependence of pulsed discharges, when regarded as sources of light, on their technical illumination characteristics (efficiency, amplitude of the light intensity, brightness, duration of the flash) on the properties of the gas discharge (type and pressure of the gas, distance between electrodes, diameter of the bulb enclosing the gas) and on the supply parameters, a picture important for practical use, was detailed in references [76,76a,128a]. It is sufficient to note at this point the principal features of this picture, and to supplement it with characteristics that are important for the understanding of the physical processes in the discharges. Data on the discharge efficiency in tubular flash lamps filled with inert gases, as can be seen from Figs. 9 and 18, are in good agreement with the corrected theoretical relationships mentioned in Sec. 2.2.3, in the region where r and E are not too large, so that re-absorption of the radiation can be neglected, and when the supply capacitor is sufficiently large (the bulk of the discharge flows after the tube channel becomes filled). At large r and E, and at sufficiently high pressures (on the order of 10^2 mm Hg), the efficiency tends to a single limit, which is the same for each given gas, and which increases somewhat with the atomic weight of the gas. In accordance with calculations, the efficiency is not dependent in this region on the initial gas pressure p (Fig. 19). The effect of the type of gas is illustrated by Table VI.

A decrease in p_0 below a definite limit, which decreases with increasing r, leads to a rapid decrease in efficiency. This can be related with the failure to satisfy the initial premises of the calculation, namely

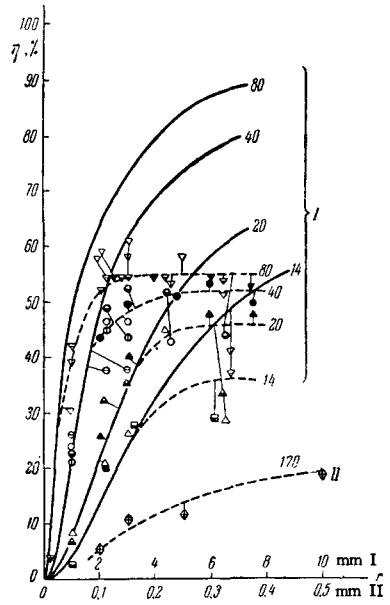

FIG. 18. Dependence of the efficiency on the internal radius of the discharge tube. Solid lines – calculated plots; dashed – average experimental curves, plotted for the following points: ◈ – E_0 = 170 V/cm; ▽ – 80 V/cm; ○ – 40 V/cm; △ – 20 V/cm; □ – 14 V/cm (the filled points were obtained with C = 600 μF; the half-filled points – with 152 μF, the open points – at 80 μF, those with vertical strokes – 48 μF, horizontal strokes – 14.5 μF, diagonal strokes – 2 μF, crosses – 0.25 μF). All the data, except the points for C = 0.25 μF, pertain to krypton at p = 100 mm Hg and l = 50 cm. The points at C = 0.25 μF pertain to xenon at C = 600 mm Hg and l = 7 cm.

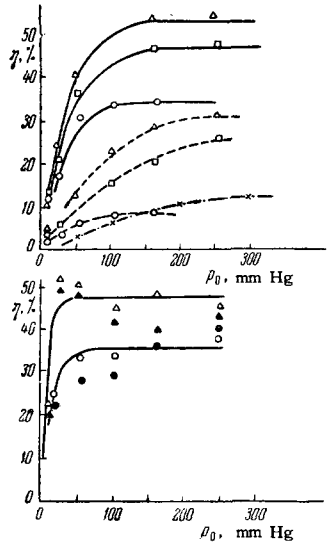

FIG. 19. Dependence of the efficiency on the gas pressure for different r_0 and EC. Upper plot: solid lines – r = 2.5 mm, krypton; dashed – 1 mm, krypton; dash-dot – 0.25 mm, xenon; △ – C = 152 μF, E_0 = 40 V/cm²; □ – 152 μF, 28 V/cm; ○ – 152 μF, 20 V/cm; × – 0.25 μF, 170 V/cm. Lower plot: r = 6.5 mm, krypton; △ – 48 152 μF, 40 V/cm; ▲ – 48 μF, 71 V/cm; o – 152 μF, 20 V/cm; ● – 48 μF, 36 V/cm.

that thermodynamic equilibrium exists in the channel, the radiation mechanisms assumed, and the energy losses on the walls. If the capacitance C is decreased below a certain value, given by

$$\frac{CU^2}{2\pi rl} \simeq 2 \text{ J/cm}^2 \qquad (28)$$

then the efficiency is decreased.

It follows from (28) that to obtain a normal efficiency there should be dissipated in a unit volume of the tube a definite energy, multiplied by the radius of the tube (a certain measure of the optical depth of the radiating layer). At values of C below that given by (28), the relative decrease in efficiency is

$$\frac{\eta}{\eta_{max}} = \left(\frac{CU^2}{4\pi rl}\right)^{0.72}, \qquad (29)$$

where C is in μF, U in kV, and r and l in cm. The notion that the discharge channel in a tubular lamp constitutes a homogeneous plasma column with a longitudinal electric gradient $U_0 - U_e/l$ (U_e –sum of the voltage drops at the electrodes, which amounts to several times 10 volts as a rule) is confirmed by the plots showing the dependence of the efficiency on l, on the basis of which the value of U_e was estimated [131,208]. It agrees also with the dependence of the flash duration τ on the parameters [207], which is approximately equal to RC/2 (R –tube resistance, C –supply capacitor) if the time constant of the discharge circuit (RC) exceeds $\sim 10^{-3}$ sec (at 35 per cent of maximum intensity; RC/2 is the power time constant of the discharge through a resistor R, in which the current varies exponentially with a time constant RC). As the discharge resistance decreases with increasing gradient of E, the value of τ likewise decreases approximately as $E^{-0.6}$. At small capacitances τ begins to change in proportion to $C^{1/2}$ and $r^{-1/2}$, this being due to the fact that the tube cross section is not filled by the discharge, and the efficiency is strongly dependent on the parameters. Inasmuch as the total energy radiated per flash is approximately equal to the product of the amplitude intensity and τ, while the brightness of the discharge filling the tube can be calculated from its intensity and from the tube dimensions, the dependence of the efficiency and of the flash duration on the parameters enables us to determine any of the technical illumination parameters of the flash. Experimental data on the amplitude brightness B of the channel can also be represented by the empirical relationship

Table VI. Comparative values of the efficiencies of tubular lamps for different gases; the efficiency of xenon is taken to be 100 [122,131]

Type of gas	r, mm	l, cm	p_0, mm Hg	C, μF	E, V/cm	Relative units
Xenon	2—7	15—100	100—150	10—1000	40—150	100
Krypton	2—7	15—100	100—150	10—1000	40—150	80
Argon	2—7	15—100	100—150	10—1000	40—150	60
Xenon	0.25	7	600	0.25	170	100
Krypton	0.25	7	600	0.25	170	55
Argon	0.25	7	600	0.25	170	16

$$\frac{B}{\left(\frac{\eta}{\eta_{max}}\right)^2} = \frac{E^{0,9}}{30} \qquad (30)$$

(B is in Gnt, the initial electric gradient E is in V/cm), where the function η/η_{max}, which differs from unity if the section of the tube is not filled with the discharge, is determined from (29).

Generalization of the technical illumination characteristics of pulsed discharges in short gas gaps, not bounded by a tube, shows that the efficiency of these discharges is practically independent of the voltage and when C exceeds ~ 0.1 μF it is independent of the capacitance C of the supply capacitor. At smaller values of C, the efficiency drops at first in proportion to $C^{1/3}$, and then even faster. The duration of the flash is proportional to the square root of the energy accumulated in the capacitor, and thus has a different dependence on C and on U.

It is noted that the efficiency and the duration of the flash depend little on the gas pressure: an increase in p_0 from 1 to 4 atm increases η and τ by approximately 1.5 times, and further increase in p_0 does not increase η or τ; the dependence on the distance between electrodes is as follows: an increase in l from 3 to 10 mm increases η and decreases τ by about 80 per cent; the dependence on the Q of the circuit is such that if the capacitor is made with insulation having larger dielectric losses, or if a ballast resistance up to 0.5 Ω is connected in the discharge circuit, the values of η and τ decrease to less than one-half; the dependence on the inductance is such that an increase in L from 0.09 to 0.22 μH decreases η by 5—30 per cent and τ in proportion to $L^{1/6}$. The influence of the type of gas in the most widely used range of discharge parameters ($C \sim 0.5$ μF, $U \sim 5$ kV, $L \sim 0.1$ μH, $l \sim 0.5$ cm, $p_0 \sim 3$ atm) is characterized by a direct proportionality between η or τ and the atomic number of the gas. At these parameters we get for xenon $\eta \cong 15$ lm/W $\cong 18$ per cent and $\tau \cong 4$ μsec. The approximate proportionality of η and τ to the atomic weight and their approximately equal dependence on the gas pressure denotes that the intensity amplitude J_a is practically independent of the gas employed; a similar independence of J_a on the type and concentration of the radiating atoms, whereas these quantities greatly influence η and τ, is observed for discharges in the vapor of a wire exploded by current [128]. In exactly the same way, the fact that η is independent of U and C (for sufficiently large C) and that τ is proportional to the square root of the flash energy leads to the same proportionality for J_a and constancy of J_a for varying C and U provided $CU^2/2$ is constant. At small values of C, the amplitude intensity decreases more rapidly than $C^{1/2}$. The opposite directions of the relatively weak dependences of η and τ on l and L leads to a more pronounced increase in J_a with increasing l and with decreasing L. J_a is particularly dependent on L in light gases and in mixtures of light and heavy gases for which dJ/dt, the slope of the leading front of the intensity, has a maximum value.

The extensive experimental material found in the literature concerning the brightness of short flashes [49,59,64,76a,106,107,187,188,198,199,201,202,204a,205,217,218] enables us to compile the following general pattern of the dependence of the amplitude brightness on different parameters, as illustrated by Figs. 20—23:*

a) In an unbounded discharge gap, the maximum (in time and in space) brightness B of the discharge increases to a definite limit ("saturates") as the gas pressure is increased, and also as the energy concen-

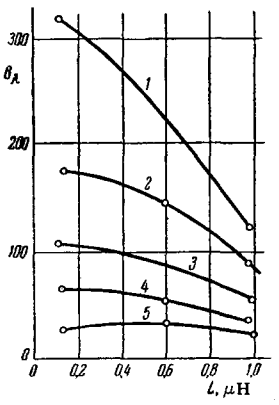

FIG. 20. Dependence of the amplitude of the spectral brightness (W/cm²nm-sr) of the radiation of discharge in argon on the inductance of the discharge circuit for different wavelengths[198]. 1 – λ = 468 nm; 2 – 554 nm; 3 – 652 nm; 4 – 723 nm; 5 – 887 nm; p_0 = 4 atm; C = 0.011 μF; U = 12 kV.

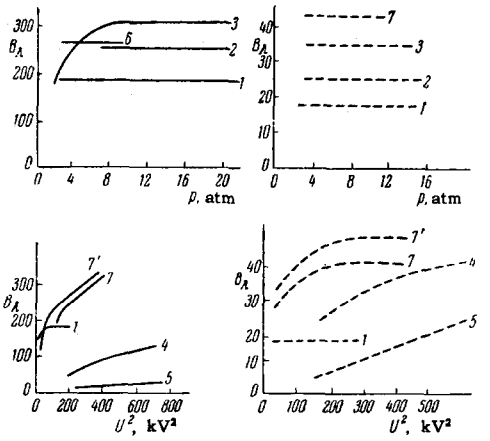

FIG. 21. Dependence of the amplitude of the spectral brightness (W/cm²nm-sr) on p_0 and U^2 in different gases[188]. Solid lines – for λ = 500 nm, dashed – for 900 nm. 1 – Xenon, 2 – krypton, 3 – argon, 4 – neon, 5 – helium, 6 – oxygen, 7 – nitrogen. C = 0.2 μF, L = 0.8 μH, U (with varying p_0) up to 26 kV, p_0 (with varying U) – 2 atm (in plot 7' – 3 atm).

*A comparison of the absolute light values B_{abs}, obtained in different investigations, allows us to assume that the values obtained in[189] are too low by about 25 per cent (possibly as a result of the large values of L), while the values obtained in [108,202] are slightly too high. The strongly overestimated values of B_{abs} obtained in [49,59,64] must be ascribed to the lack of exact correction of the spectral sensitivity of the measuring photocell against the standard visibility curves, and possibly to other measurement errors.

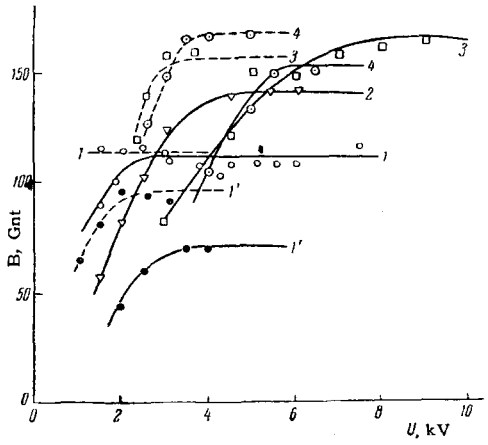

FIG. 22. Dependence of the amplitude of the light brightness (Gnt) on the supply voltage[76a]. 1 – 5 mm, C = 0.5 μF, L = 0.2 μH (continuous lines) and 0.02 μH (dashed). 1 – xenon, p = 3 atm (1′ = 0.66 atm); 2 – krypton, 3 atm; 3 – argon, 3 atm; 4 – mixture of 66% (at) xenon + 26% (at) nitrogen.

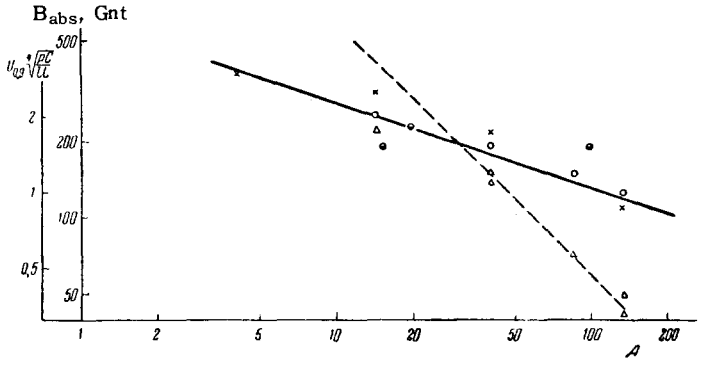

FIG. 23. Dependence of the absolute brightness limit (continuous line, where the light circles are the data of [76a], the half-filled circles pertain to gas mixtures, and the crosses are the data of [108,202]) and the supply voltage at which $B = 0.9B_{abs}$ (dashed line, triangles,[76a]) on the atomic weight.

tration in the space and in time is increased by raising the working voltage and reducing the inductance of the discharge circuit and the distance between electrodes.

At pressures up to several atmospheres, the saturated value $B_{sat}(p)$, reached at a definite energy concentration, increases with the pressure, and at larger pressures it ceases to depend on p. In exactly the same manner, the saturated value $B_{sat}(\mathcal{E})$ reached at a certain pressure first increases with increasing energy concentration, and then becomes independent of the latter. By the same token, a characteristic absolute limit of discharge brightness B_{abs} exists for each gas.

b) For gases with smaller atomic weights, the value of B is lower at small pressures and energy concentrations than for the heavy gases. However, the value of B_{abs} is attained in the latter at lower values of p and at lower energy concentrations than in light gases. Further increase of the pressure and the concentration cause the brightness of the discharge in light gases to overtake the brightness of the discharge in heavy gases, which stops increasing. The absolute discharge brightness limit thus increases with decreasing atomic weight A of the gas approximately as $A^{-1/3}$. The supply voltage $U_{0.9}$, at which B reaches a value $0.9\,B_{abs}$, is approximately proportional to A^{-1}, and also to $L^{1/4}$, $C^{-1/4}$, $p_0^{-1/4}$, and $l^{1/4}$. Mixtures of gases, such as air, have somewhat anomalous values of B_{abs} and $U_{0.9}$.

c) The spectral brightness of the discharge attains its limit in the long-wave region much earlier than in the short-wave region.

One of the proposed explanations for the described pattern is that when the energy concentration in the gas is high, the energy is "locked" for some time inside the opaque channel whose outside layers are at the limiting temperature reached in this gas. This assumption agrees, as it were, with the fact that in a discharge bounded by a capillary tube, in which the small optical depth of the radiating layer should cause the "locking" of the radiation to be less, higher brightnesses are attained than in an open discharge (in [205] values B = 500 Gnt and T_{br} = 94,000°K were obtained in a discharge in a capillary 0.4 mm in diameter and 10 mm long at an air pressure 1 atm, capacitor rating 0.011 μF, and voltage 29 kV).*

However, such an explanation, which calls for the existence of considerable temperature gradients within the confines of the conducting column of the discharge, contradicts the temperature measurements made by an interference method[31], and also the lack of self-inversion of the lines of ionized atoms (in portions of the spectrum in which the presence of the lines proves that the continuous background has not yet reached the brightness of an absolutely black body)[108,201] and the equality of the brightnesses observed on the end and perpendicular to the axis of the capillary discharge[106, 204a]. This suggests a second explanation for the saturation in the growth of the brightness, namely that for each gas the "effective specific heat" of the plasma, which accounts for the energy consumed in ionization, channel expansion, and radiation increases at a definite temperature at so steep a rate, that further appreciable increase in T would call for an increase in the energy concentration in discharge, something difficult to attain in practice. One can assume that the observed singularities in the values of brightness for gas mixtures will find an explanation when the "effective specific heat" of the channel is finally calculated.

4.2. Estimates of the Transparency and Temperature of the Channel

In connection with the high temperature of the channel, its radiation, including that with continuous spec-

*Analogous conclusions concerning the "locking" of the radiation are drawn from a measurement of the high temperatures in strong shock waves produced in a gas by chemical explosions[136].

trum, should experience noticeable re-absorption, the degree of which is an important characteristic of the plasma. If the electric gradient and the energy concentration are very large, the coefficient representing the absorption of its own radiation by the plasma is a very large quantity. This follows from the observed almost complete equality of the measured brightness of short discharges and the calculated brightness of an absolutely black body; the corresponding measurements were made in greatest detail by Vanyukov, Mak, et al on high-intensity discharges in capillaries [106,108,205] and unbounded gaps [197-201]. To the contrary, in the case of small electric gradients, which occur in the case of prolonged discharges in tubular flash lamps, the coefficient of own-radiation absorption should be small. This follows from the agreement between the corresponding experimental values of the efficiencies of such lamps with those calculated without account of absorption (Figs. 9 and 18).

Direct experimental measurements of the absorption of light in a spark discharge were made by Laporte and Gans [86,88,90], Gurevich [68a], Calker [18], Fischer [49], and Marshak [125]. Laporte, working with a tubular xenon flash lamp of rather low pressure (~ 5 mm Hg) at a gradient ~ 60 V/cm and very small supply capacitor (to 2μF), estimated this coefficient to be less than 0.015 cm^{-1}. At a larger gradient (~ 220 V/cm) values of ~ 0.1 cm^{-1} were obtained in the red and green parts of the spectrum, and reached 0.2 cm^{-1} in the blue part. Gurevich obtained for a spark discharge in air at 7—9 kV and with a supply capacitor of several microfarads a much larger coefficient of absorption.* Calker presented a qualitative description of absorption of light during the final stage of a spark discharge in air containing metal vapor as an admixture.

Fischer, working with a powerful low-inductance discharge circuit (L = 0.035 μH, C = 2.75 μF) found that the transparency of the channel relative to its own radiation (reflected by a mirror) decreased below 20 per cent for a discharge in argon at 2.5 atm and ~ 12 kV/cm and for a discharge in helium at 2.8 atm and 23 kV/cm. From the data on channel expansion given in Sec. 3.3 we can estimate that the coefficient of absorption corresponding to this value of transparency exceeds 10 cm^{-1}. According to Fischer, the absorption of the channel is approximately the same over the wavelength range from 250 to 450 nm.

The coefficient of absorption μ in tubular flash lamps with flash durations 10^{-3}—10^{-4} sec, integrated over the time and over the spectrum, was determined in [125] by measuring the angular distribution of the radiation intensity. This method was used previously for similar purposes by Fabrikant, Pul'ver, Safraĭ, and Aronovich [44] and by Laporte [86,88]. Comparison of the relative intensity with that of a pure volume radiator made it possible to calculate μ by means of formulas derived by Gershun [63a]. The plot of μ vs. the initial electric gradient (Fig. 24), obtained in [125], shows that under the conditions prevailing in tubular lamps the integral absorption coefficient lies between 1 and 2 cm^{-1}.

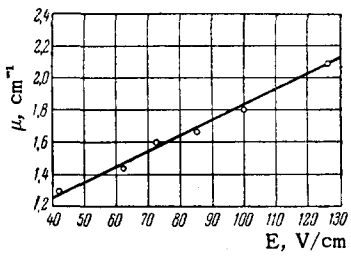

FIG. 24. Dependence of the absorption coefficient in tubular flash lamps on the initial electric gradient. (l = 50 cm, r = 2.5 mm, krypton, p_0 = 150 mm Hg, C = 36-320 μF).

In addition to reabsorption of radiation, extensive information on the state of the plasma can be gained from the spectral characteristics of the radiation.

The spectral distribution of all the energy radiated by a pulsed discharge per flash was described by Laporte and his coworkers [90], and also by many other authors [4,5,66,76b,77,141,149,154,172,213a]. It is characterized by lines (from arcs and from multiply and singly ionized atoms)* superimposed on a continuous background. The background is due to the appreciable broadening of certain lines, owing to the interaction between atoms in the discharge, and also to recombination and "continuum-continuum" transitions, including the so-called "pseudo continuum," formed by the coming together of the terms near the ionization boundary as a result of their broadening. The relation between the line intensities and the background [90] depends on the concentration of the energy in discharge and on the kind and pressure of the gas; the background becomes stronger with increasing discharge power and decreasing tube diameter and also with increasing atomic weight and pressure of the inert gas.† The background plays a more noticeable role in the ultraviolet and visible zones of the spectrum, and is much more weakly pronounced in the infrared zone. Typical relations between the shares of the energy going to these zones, are listed in Table VII. [213a]

A change in the supply capacitor by one order of magnitude and a two-fold change in the supply voltage hardly influence the spectral distribution of the energy of tubular lamps, with an appreciable change occurring only, for example, when the initial electric gradient is increased from 25 to 210 V/cm. The relative distribution of energy among the bands is likewise weakly

*Gurevich does not give the absolute values of the coefficients, which are usually expressed in reciprocal centimeters.

*Lines not excited in the less intensive discharges in the same gases, including those corresponding to "forbidden" transitions, are also observed.

†At pressures above ~10 mm Hg, bright lines reappear against an intense background, and increase the light yield of the discharge. They are also stronger in the case of the narrowest tubes, owing to the small depth of the radiating gas layer.

Table VII. Fractions of energy radiated by different pulsed discharges in the ultraviolet (230—400 nm), visible (400—700 nm) and near infrared (700—1000 nm) bands of the spectrum (in per cent relative to $CU^2/2$)

Radius of bulb, mm	Distance between electrodes, mm	Gas	p_0, mm Hg	U, kV	C, μF	Fraction of the energy		
						Ultraviolet	Visible	Infrared
2.5	70	Xenon	100	0.3	2500	3	18	30
2.5	70	»	100	1.6	8	15	11	32
2.5	70	»	100	0.12	5800	—	13	35
0.25	70	»	600	1.2	0.25	—	7.2	15.5
0.25	70	Krypton	600	1.2	0.25	—	4.2	2
0.25	70	Argon	600	1.2	0.25	—	1.2	2.6
12.5	2.5	Xenon	2300	3	3	21	7.8	22
12.5	2.5	»	2300	3	0.27	4.5	5.9	5.5
12.5	2.5	»	2300	3	0.025	4	5.5	6.5

influenced by the diameter of the tubular lamp and by the gas pressure, but it is appreciably dependent on the type of gas. For spherical lamps with a short spark gap an increase in the supply capacity by several microfarads has a rather strong effect on the distribution of energy among the bands.

In addition to studying the spectral distribution of the total energy radiated by the discharge during the entire flash, many investigations by Bogdanov and Vul'fson [13,14,215], Mandel'shtam and his co-workers [112,115,116,192] and Vanyukov, Mak, et al [9a,106,108,197-199,203-205,205a] were devoted to spectra of the pulsed discharge at various instants of time.

It was established in [13,14,44a,115,116,179a,192,203,204,205a,215] that individual spectral elements (arc lines, lines of singly and multiply ionized atoms, continuous background), which have different excitation energies, are shifted relative to one another in time in accordance with the change in channel temperature during the course of the discharge. Figure 25 shows examples of time plots of the intensities of different lines and of the background, obtained in [115,192]. The left-hand plot, which pertains to air at atmospheric pressure, shows that in the earliest stage of the discharge the most intense are the lines of the doubly ionized atoms, and that the intensity of the continuous background reaches a maximum somewhat later, followed by the maxima in the lines of the singly charged ions

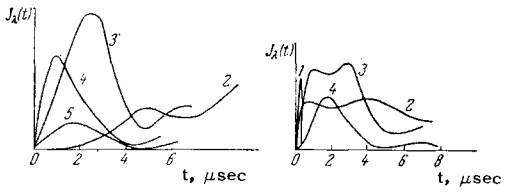

FIG. 25. Variation of the intensities of the different spectral elements during the time of the discharge. 1 – Nitrogen molecule band; 2 – H_α line of hydrogen; 3 and 4 – lines of singly and doubly ionized nitrogen atoms; 5 – continuous background. Left – air, 1 atm, 0.25 μF, 10-15 kV, 10 μH;[192] right – commercial nitrogen, pressure lower than 100 mm Hg; the remaining parameters are the same.[115] (The abscissas represent the time t in microseconds.)

and finally by the maximum of the arc spectrum. The right-hand plot, obtained for nitrogen at reduced pressure (when the vigorous growth in current density becomes stretched out, see Sec. 2.2.1 and [84]), makes it possible to trace the change in the spectrum not only during the drop in temperature following the maximum of the electric power of the discharge, but also during the course of the rise in temperature. At the very start one observes here the molecular bands of nitrogen and weak lines of the neutral atoms, followed by the first maximum of the spectrum of the singly-charged ions, and then by the doubly charged ions (temperature maximum), followed still further by an alternation of the maxima in reverse order.* Figure 26a shows for three different discharge modes how the time required for the line intensity to reach a maximum varies with increasing excitation energy $\mathcal{E}$ of the upper level of the line; in this case we are considering the decrease in temperature following the maximum of the electric power.

Using the fact that for a given discharge mode the experimental points for all lines with different excitation energies fit on a common plot, we can find on this plot the point with an abscissa equal to the time required for the background to reach maximum. The ordinate of this point can be assumed to be the "effective excitation energy of the continuous background," which turns out to lie between 55 and 45 eV for different discharge intensities. It follows therefore that triply or doubly charged ions play a noticeable role in the formation of the background, which is produced principally by the bremsstrahlung of the electrons and by recombination.

If it assumed that the level population is proportional, in accord with the Boltzmann formula, to $\exp(-\mathcal{E}/kT_e)$, where T_e is the electron temperature and k Boltzmann's constant, then the intensity of the

*The plots on Fig. 25 pertain to oscillating discharges, this explaining the repeated increase in all the intensities after 5 microseconds (after the start of the second half wave of the discharge).

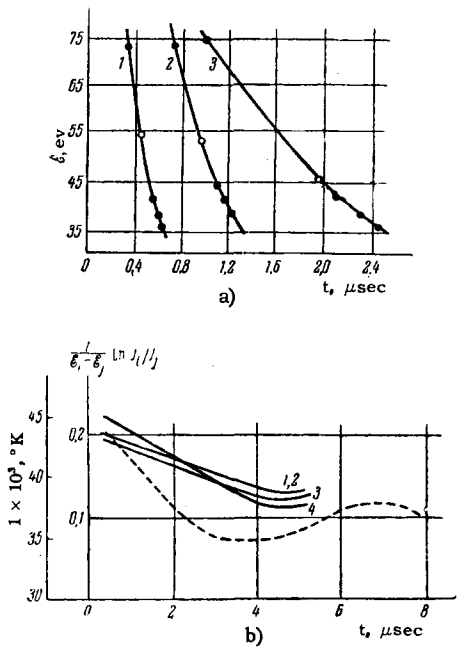

FIG. 26. Parameters of line spectrum of a short discharge in air[192,112] (1 atm, U_0 = 10-15 kV). a) Dependence of the time necessary for the nitrogen lines (dots) and for the background (circles) to reach maximum intensity on the excitation energy of the upper level. 1 – 0.01 μF, 10 μH; 2 – 0.25 μF, 2.6 μH; 3 – 0.25μF, 10 μH: b) time variation of the logarithm of the ratio of intensities of different pairs of lines (the solid curves are aligned for the instant 2.5 μsec) and the temperature calculated from this ratio (curve 1) (dashed curve); 0.25 μF, 10 μH; the numbers on the continuous curves correspond to the following:

No. of curve	λ_i, nm	$\mathscr{E}_i$, eV	Spectrum	λ_j, nm	$\mathscr{E}_j$, eV	Spectrum
1	409.7	74	N III	399.5	35.5	N II
2	517.9	44.5	N II	504.5	35.5	N II
3	553.5	41.5	N II	549.5	47.5	N II
4	549.5	47.5	N II	460.7	35.5	N II

i-th spectral line with frequency ν_i is*

$$J_i = \frac{g_i}{g_0} h\nu_i A_i N_0 e^{-\mathscr{E}_i/kT_e}, \qquad (31)$$

where g_i and g_0 are the statistical weights of the upper and lower levels, A_i the transition probability, and N_0 the concentration of the atoms or ions in the unexcited state.

Accordingly we have

$$\frac{1}{\mathscr{E}_i-\mathscr{E}_j}\ln\frac{J_i}{J_j} = B_{ij} - \frac{1}{kT_e}, \qquad (32)$$

where B_{ij} is a constant characterizing a given pair of lines and independent of the temperature.

Consequently the temperature variation and hence the time variation of the quantity $\frac{1}{\mathscr{E}_i-\mathscr{E}_j}\ln\frac{J_i}{J_j}$ should be the same for any pair of lines, accurate to a certain constant. Figure 26b, taken from [192], confirms this conclusion, and by the same token confirms the assumed existence of a definite temperature and of a definite Boltzmann level population.

On the basis of the measured line intensities over the extent of the flash and on the basis of formula (31), for which the transition probabilities were calculated, and also on the basis of the Saha formula, the electron temperature of the discharge plasma was determined in [108,112,116,179a]. Under the discharge conditions indicated in the caption to Fig. 26b, the three pairs of lines denoted by the numbers 1, 2, and 3 in this caption, have given for the instant t = 0.5 sec an estimate of 43, 38, and 52 thousand deg K respectively for the electron temperature.

In [108], temperature values 26—33 thousand deg K were obtained from four pairs of lines under much harder discharge conditions (0.05 μF, 2—8 kV, 0.1—0.04 μH). The average of the estimates obtained in the foregoing investigations, 35,000°K, is in satisfactory agreement with the gas temperature estimate T_{gas} = 40,000°K, obtained in investigations of the channel expansion and of its electrical characteristics (see Chapters II and III), and also from brightness measurements (see below). By the same token, the experiment has confirmed the theoretical conclusion [112,113,116] that thermodynamic equilibrium is established in the pulse discharge channel quite rapidly and that the Boltzmann and Saha formulas are applicable in this case.*

Figure 26b shows also the time variation of the channel temperature, calculated by the method described above from measurements of the variation of the spectral line intensities. What is striking is the relatively small range of temperature variations corresponding to a considerable change in power and discharge intensity. This fact is still another argument in favor of attributing the limiting brightness to the sharp increase in the "effective specific heat" of the channel (see Sec. 4.2.4). Table VIII lists the results of the calculation [112] of the degree of ionization of nitrogen at several temperatures, and explains clearly the predominance of the N III spectrum at the instant of the temperature maximum and the subsequent increase in the N II spectrum.

A completely independent estimate of the discharge temperature can be obtained by measuring the absolute values of the spectral brightness of the channel at so high an energy concentration as to make the brightness reach its limit. The spectral distributions of the brightness of the continuous background in the visible and near infrared regions were measured in [197,198,205] at different stages of the discharge. These measure-

*We consider here lines which do not experience reabsorption. The criterion used in [192] for absence of reabsorption was that the relative intensity of the multiplet lines remain constant over the extent of the discharge.

*A cautious estimate[112,116] yields for the time necessary for a stationary distribution of excited atoms and ions to be established a value $\lesssim 10^{-10}$ sec, while the time necessary to establish stationary ionization is $\lesssim 10^{-7}$ sec.

Table VIII. Concentration of neutral, singly and multiply ionized nitrogen atoms at different temperatures [112]

T, 10^3°K	N, %	N^+, %	N^{++}, %	N^{+++}, %
20	1	98.7	0.3	—
30	0.03	50	50	—
40	—	4	93	3
50	—	0.4	61	38.6
60	—	0.02	10	90

ments have shown that for a discharge not bounded by a capillary and for a sufficiently high energy concentration (low inductance, high pressure and supply voltage, first instants of the discharge), at which brightness saturation is reached, the yield B_λ of the discharge agrees well with the variation of B_λ of an absolutely black body with a temperature of 27,500°K in the case of xenon. For discharges in capillaries, and also for unbounded discharges in air when the experimental conditions did not result in brightness saturation, the plots of B_λ of the channel could not be superimposed with sufficient accuracy on the plots of B_λ of an absolutely black body with suitably chosen temperature. The agreement between the B_λ plots for xenon and those for an absolutely black body has made it possible to assume that under these conditions the channel discharge in this gas had the corresponding temperature.

A more precise approach to an estimate of the temperature by measuring the spectral brightness was made in [108,200-202]. In these investigations B_λ was determined not only on the continuous-spectrum portion, but also in the center of gravity of the broadened lines, in which the brightness saturation occurs under conditions that are much softer than the mode necessary to saturate the background. A sign that B_λ of the line and of an absolutely black body are equal is the broadening of the line resulting from the fact that its center "leans" as it were against the limiting brightness at the given temperature, and the "skirts" "overtake" the middle. The results of the described method of determining the temperature for different gases are shown in Fig. 27. This figure shows that the estimate obtained for T of air (38,000°K) is in satisfactory agreement with the estimate obtained by other methods. An estimate of T of xenon agrees with the estimate

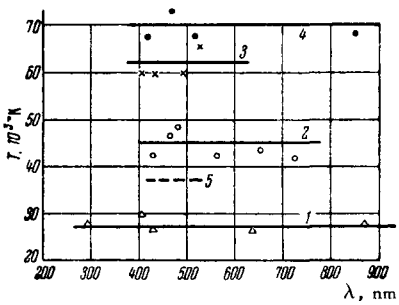

FIG. 27. Temperature values calculated from the maximum values of B_λ in different continuous and line radiation regions of the spectrum.[108] 1 – Xenon; 2 – argon; 3 – nitrogen; 4 – helium; 5 – air.

obtained in [197,198] by measuring the B_λ of the continuous background.

The pattern of the spectral distribution of the energy radiated during the entire flash was supplemented in [108,109,203,204,205a] with data on the spectral distribution of the radiation power at different instants of the flash, the first four references pertaining to the wavelength range 250—550 nm, and the fifth to 500—1000 nm. In addition to the difference in the phases of the occurrence and disappearance of the lines with different upper-level excitation energies, a fact disclosed already in earlier investigations, the later investigations have shown that even at the instant of maximum discharge power the ultraviolet spectrum of the radiation, including the continuous background, is not at all similar to the spectrum of an absolutely black body. The corresponding instantaneous spectral distribution of the power does not differ strongly from the spectral distribution of the energy radiated over the entire flash under the same discharge conditions. At the same time, attention should be called to the fact that the spectrum approaches an equal-energy distribution at the instants that follow the maximum of the power, and that the continuous background is reduced even during the instant of maximum power when the absolute values of the maximum power are made small by an inductance in the discharge circuit.

Of certain interest are the data obtained in [108,204] on the broadening and shifting of certain spectral lines at instants close to the maximum of the discharge power. These data show that under the influence of rather large intermolecular fields certain lines become broader by several nm, and that as a result of the quadratic Stark effect they shift into the red or blue side (depending on the sign of the Stark-effect constant) by 1—2 nm. Calculation methods customarily used in spectroscopy have yielded for the measured broadenings and shifts electron concentration estimates on the order of $N = 10^{18}$ cm^{-3} (helium, 15 atm, 9 kV, 0.18—1 μH). Another estimate of N was obtained in [108,109] on the basis of measurements of the intensity of the continuous background of a discharge in helium (Fig. 28). The values obtained in this case were approximately three times larger. The obtained values of N made it possible [108,109] to estimate with the aid of hydrodynamic relations once more the temperature of the channel. The values of N obtained from the line broadening yield temperatures of 100,000 —200,000°K for the discharge in helium, while the values of N determined from the intensity of the continuous background yield values of 45,000—70,000°K.

V. NEAR-ELECTRODE PHENOMENA

The physical phenomena occurring in the near-electrode regions of a pulse discharge have not yet been sufficiently clearly represented to be able to derive the practical laws that are essential to make this

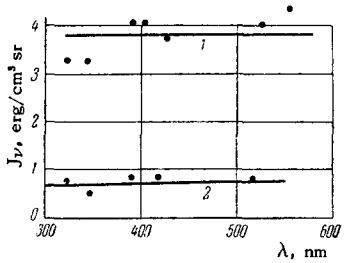

FIG. 28. Dependence of the intensity J_ν (per unit interval of frequency ν and per unit volume) of the continuous background of a discharge in helium on the wavelength[109]. p_0 = 15 atm, U_0 = 5 kV, time after start of the discharge (in microseconds): 1 – 0.1 (L = 0.18 μH); 2 – 0.2 (L = 1 μH). J_ν was determined by dividing the spectral brightness of the channel by its diameter, it being assumed here that the channel is transparent.

discharge usable for pulsed light sources. However, in view of the relatively isolated nature of the near-electrode processes in the principal channel of the discharge and in view of the fact that in most cases they are not of primary significance for practice (the principal external manifestations of the discharge are determined by its channel), the lack of sufficient development in the physics of the near-electrode phenomena has at first been little felt. Only the rapid progress in the technical application of pulsed light sources has recently attracted the attention of many investigators to near-electrode phenomena.

The special complexity of these phenomena lies in the fact that along with the radial-temporal inhomogeneity of the discharge channel we are dealing here also with a longitudinal inhomogeneity, together with a whole series of additional mutually related physical processes in the boundary layer between the gas and the metal and within the metal itself. Among these processes one can mention in first order the following:

a) Ionization of the gas in the near-electrode regions, formation of near-electrode space charges, and emission of electrons from the cathode; these processes determine the energy fed to the electrodes (near-electrode losses, which influence the efficiency of the discharge) and the conditions under which the electrodes are bombarded by the plasma particles.

b) The distribution of heat in the electrodes and the melting and evaporation of the electrode metal, which determine directly the technically second most important (following the efficiency) manifestation of all the near-electrode processes, namely the sputtering of the electrodes and the resultant darkening of the flash lamp bulb, which usually limits its lifetime.

All these processes are so complicated that at the present time there are still no general theoretical descriptions of even stationary arc discharges. Moreover, the intermittent (in space and in time) character of the phenomena on the cathode of the stationary arcs has caused a study of the near-electrodes regions of the arc to follow the line of experiments with pulsed discharges, and at the present time the investigations of the near-electrode regions of stationary and pulsed discharges are being carried out on a practically unified front.

In view of the highly imperfect state of these researches, it is advantageous to summarize here briefly the main available information on near-electrode phenomena.

Observations of the cathode spot, made with the aid of a Kerr shutter with an electron-optical converter, using markers placed on the cathode, etc,[15, 24,33,56-58,114,116,152,169,175,176,220] have shown that the spot has a multiple structure. Its structural element is a microregion 5—10 μ in diameter, producing in the discharge a current of about 0.5—5 A. Such a microspot, in which the current density ranges from several times 10^5 to 10^7 A/cm², stays in one definite place for a very short time (~ 0.1 μsec). Between the glowing zone of the microspot and the cathode there is a dark space ~ 0.1 mm wide, and therefore the current density on the cathode itself may be even higher. In the case of a perfectly homogeneous surface (mercury cathode) the spot moves smoothly with a speed ~ 10^4 cm/sec, stretching into an arc segment with increasing current. The current density remains constant, and if the rate of current growth dJ/dt is sufficiently steep, the arc assumes a circular or semicircular form (the latter if the initial spot has occurred on the edge of the cathode). If dJ/dt is so large that the increase in the active surface resulting from the increase of the radius of the arc becomes insufficient, then new microspots occur on the side, from which similar arcs then propagate. In the case of an inhomogeneous surface (contamination, crystalline structure) the microspots move in jumps, and concentrate on the inhomogeneities. The average rate of displacement of the spots along the cathode surface is on the order of 10^5 cm/sec. The number of microspots in this case is apparently[24,57,116] equal to the total discharge current divided by the current of one spot (~ 5 A). On the whole the aggregate of spots encloses with increasing current and with broadening channel a rather appreciable zone of the cathode surface.

The formation of microspots is connected with the occurrence of emission centers. This can be attributed to the combined action of the thermionic and field-emission mechanisms[92-94]: under the influence of the energy delivered to a small region on the cathode, this region becomes heated and the population of the high energy levels increases in the electron gas of the metal, and consequently field emission with a current density ~ 10^6 A/cm² becomes possible at the electric field ~ 2 × 10^7 V/cm which can be produced near the cathode by the space charge when the current density has this value. The corresponding estimated temperature of the heated region (3000°K with allowance for the roughness factor and 3500°K without this factor) is quite realistic[23] for cathodes made of copper and metals with higher melting points. At the same time,

in the case of a mercury cathode the more likely is a mechanism [42,155], the authors of which believe it to be likewise applicable to copper, namely that the atoms are excited in the vapor cloud resulting from the local heating, and by returning to the main bulk of the metal within a short time, during which they have no time to emit a photon, they give rise to electron emission similar to the emission produced under the action of the metastable particles in the Townsend discharge ("epsilon" process).[126] Such a mechanism is confirmed by an approximate calculation based on an estimate of the number of returning atoms, $\sim 10^{25}$ atoms/cm^2-sec (experiment yields for the amount of evaporated mercury a value 3×10^4 g/C, that is, 10^{24} atoms/cm^2-sec;* the ratio of the number of returning atoms to the number of those leaving the cloud can be 10 : 1), which at $\epsilon \sim 1$ yields an emission current density $\sim 10^6$ A/cm^2. It is possible that the high current density in the microspot is due to its own magnetic field which acts on the ionized vapor.

The appreciable amount of energy released in the microspot leads to an instantaneous evaporation of a definite amount of metal, accompanied by an explosion-like propagation of vapor. Experiment [70,114] has shown that jets from solid cathodes have a discrete structure which agrees with the discrete structure of the cathode microspots (time of emission of one jet is on the order of 10^{-7} sec and is equal to the lifetime of one spot).

The explosion of a microspot is analogous in some sense to the explosion produced under the influence of a condensed electric discharge in a thin metallic wire [3,30,43,85,128]. Just as in the explosion of an electric wire the electric current is interrupted at the first instant because of the large current density (and resumes only after the vapor has expanded), so does the flow of current at the given point of the cathode become impossible during the explosion of the microregion on the cathode. This, apparently, is exactly why the center of emission moves to neighboring portions of the cathode. Such a mechanism is confirmed, for example, by the agreement between the rate of propagation of the shock wave, calculated on the basis of the hydrodynamic theory (see Sec. 3.2), and the average rate of displacement, along a filamentary electrode, of pulsed microdischarges † of a relaxation circuit (capacitance on the order of 100 pF, charging resistance on the order of 1000 Ω) experimentally obtained by Boyle [15].

The explosion-like character of the eruption of vapor from the cathode is confirmed by the spectroscopic investigations of the torches produced on cathodes made of alloys [151], and also the absolute measurements of the speeds of the streams [70,114,116,169]. The former have shown that if the cathodes are made of metal alloys, the velocities of the different atoms in the vapor jets are the same, and the latter have shown that the velocities of the jets amount to 10^5—10^6 cm/sec. These rates change in accordance with the changes in the discharge current and are inversely proportional to the atomic weight of the cathode metal, so that the kinetic energy of the atoms in the jets from cathodes made of different metals turns out to be the same if the discharge conditions are the same [114,169].

Several attempts to calculate the evaporation of the metal contained in the vapor jet have been reported in the literature [100,114,176]. These calculations are based on some estimate of the energy delivered to the metal from the adjacent region of the channel (in [100] the estimate made of the ion current is obviously too low and it is assumed that each ion is capable of recombining, owing to the tunnel effect, and of transmitting excitation energy to the metal; in [114,116,176] the energy is estimated as the product of the current density, determined from the current oscillogram and from the dimensions of the microspot, by the tentative magnitude of the voltage drop, ~ 10 V, and by the time interval between the eruptions of the individual jets, which is approximately 1 microsecond*), and on an estimate, made by solving the heat conduction equation, of the depth of the metal zone around the cathode spot, within which the temperature reaches the melting point (in [100]) or the boiling point (in [114,116]).

As a result of these calculations, based on different initial data, one obtains the same order of rate of evaporation of the metal ($\sim 10^{-2}$ g/sec), which agrees with experiment. The differences in the initial premises (in [100] even the multiple structure of the cathode spot is disregarded) and in the experimental conditions do not allow us, however, to assume thus far that this agreement is a convincing confirmation of the theories, an agreement which would permit us to use the calculation methods for practical purposes. Thus, the results of the calculations are more likely to serve as an illustration of the applicability of the physical hypothesis on which they are based.† A similar illustration is the estimate made in [114,116] of the energy balance in the cathode spot (of the 10 cal/cm^2 arriving in the spot, 1 cal/cm^2 is dissipated in the metal by heat conduction, 3 cal/cm^2 are consumed in evaporation, and 6 cal/cm^2 are converted into kinetic energy of the jet) and the vapor pressure of the

*This agrees with the data of Libin[100] for low-melting-point cathodes, according to which the amount of evaporated lead or bismuth amounts to 4×10^{-4} g/C.

†Boyle[15] relates the occurrence of the discharge with the displacement of a region of reduced density behind the shock-wave front; in this region the distance between the very closely located electrodes corresponds to the minimum of the Paschen curve.

*So large an interval is obtained with a discharge circuit of appreciable inductance ($L \geq 100$ μH). At smaller values of L the individual jets are superimposed on one another.

†It should be noted that at the present time no fully reliable calculation has been made of even the much simpler case of instantaneous evaporation of metal during the explosion of a wire [30,43,85].

Table IX. Average rate of evaporation in pulsed discharges of cathodes made of different pure metals [100] (discharges in argon, 500 mm Hg, l = 4 mm, cathode diameter 2.5 mm, C = 3 μF, U = 250 V, ballast resistance 1 Ω, frequency 50 cps)

Cathode material	Units	Be	Al	Mo	W	Cu	Ag
Average value of specific heat capacity used for the calculations	cal/g-deg	0.6	0.32	0.08	0.042	0.15	0.086
Calculated velocity *)	10^{-7} g/sec	4.3	16	16	23	20	40
Observed velocity **)	10^{-7} g/sec	3.0	12	14	14	17	27

Cathode material	Units	Zn	Cd	Sb	Sn	Pb	Bi
Average value of specific heat capacity used for the calculations	cal/g-deg	0.14	0.080	0.098	0.080	0.039	0.058
Calculated velocity *)	10^{-7}g/sec	56	130	54	180	260	210
Observed velocity **)	10^{-7}g/sec	55	91	91	200	340	380

*The absolute calculations were made in [100] by substituting in formula (33) the following expression for the overall energy dissipated on the cathode per second: $\mathcal{E} = fCUV_i\sqrt{m_e/m_i}$ (f – flash frequency, V_i – ionization potential of the gas, m_e and m_i – masses of the electron and of the ion), obtained from the assumptions mentioned above.

**If it is assumed that the reciprocal of the duty cycle of the pulses amounted to $\sim 5 \times 10^3$ in [100b] (this corresponds to a real effective current pulse duration ~4 μsec), then the average rate of evaporation listed in the table, 20×10^{-7} g/sec, corresponds to a rate of $\sim 10^{-2}$ g/sec during the time of the current pulse.

metal erupted from the cathode (~ 100 atm), which determines the occurrence of the explosive wave. The hydrodynamic nature of the torch, the temperature of the vapor in which is 2000—3000°K, agrees with the thin layer of dark space between the surface of the cathode and the brightly glowing zone of the microspot, observed in [114,116]. The bright zone of the microspot is obviously a vapor cloud heated by the discharge, after covering a path of ~ 0.1 mm, to the plasma temperature of 20,000—40,000°K. [114,116,181a].

The relative values of rates of evaporation of different metals, calculated in [100], appear to be more reliable. By solving the heat conduction equation for a mass M of metal enclosed in the melting zone when an energy $\mathcal{E}$ is instantaneously released at a point on the surface, we obtain the expression

$$M = 0.3\frac{\mathcal{E}}{\gamma T_0}, \qquad (33)$$

where γ is the relative specific heat of the metal and T_0 its melting temperature.

The use of this formula would be justified were the energy released on the cathode to be independent of the cathode material (this obviously should not take place if the difference in the work function is large) and were the amount of metal expelled independent of the latent heat of melting and heating the metal to evaporation. The satisfactory agreement between the relative values of the rates of evaporation, obtained for different pure metals from formula (33) and from experiment (see Table IX) shows that these assumptions are feasible; for activated cathodes this formula does not yield a correct estimate of M.

Under the specific experimental conditions of measurement of the rate of evaporation of cathodes as used in [100], a strict proportionality was observed between the evaporated substance and the amount of electricity passing through the discharge (with variation of the supply capacitor, the working voltage, and the ballast resistance, the latter up to 7 ohms). For most conditions encountered in flash lamp design practice, however, such a proportionality is not observed at all [206] and the dependence of the rate of sputtering on the foregoing parameters is rather complicated. One reason for it is that formula (33) derived for the case of an instantaneous and point-like release of energy on the cathode, cannot be extended to include discharges with relatively long pulse duration and large simultaneously operating cathode zone. Second, one cannot expect the energy released from the cathode to be proportional to the quantity of electricity flowing through the discharge if the discharge conditions are appreciably varied.

We have delineated in broad outlines the presently available picture of processes occurring on the cathode of a pulsed discharge. Since the darkening of the bulb of the flash lamps is primarily due to the sputtering of the cathode (assuming that the anode is sufficiently large not to become heated as a whole to the temperature of intense sublimation of the metal, the anode is

hardly sputtered at all in flash lamps) and that it is the cathode that influences the efficiency of the discharge, the phenomena on the anode are of lesser practical interest. They reduce briefly to the contraction of the channel into one common spot, in which, under ordinary conditions, there is a continuous and quieter evaporation of the metal (without explosions and with a smaller rate of flow than on the cathodes). With broadening of the discharge channel, the anode spot also broadens [177]. The current density in it amounts to about 10^5 A/cm^2. The anode drop, estimated from the thermal effects [12] (determination of the thickness of the foil melted during the course of the discharge, with subsequent calculation of the propagation of the heat, analogous to that used for the cathode), amounts to 2—9 V.

[1] I. S. Abramson and N. M. Gegechkori, JETP **21**, 484 (1951).

[2] Abramson, Gegechkori, Drabkina, and Mandel'shtam, JETP **17**, 862 (1947).

[3] I. S. Abramson and I. S. Marshak, ZhTF **12**, 632 (1942).

[4] J. N. Aldington, Endeavour **7**, 21 (1948).

[5] J. N. Aldington and A. J. Meadowcroft, JIEE **95**, pt. II, 671 (1948).

[6] K. Ando and B. Matsuoka, Mem. Ehime Univ. **3**, 1 (1955).

[6a] K. Ando and K. Takahahi, Mem. Ehime Univ. **4**, 11 (1960).

[7] S. I. Andreev and M. P. Vanyukov, Paper delivered to the Second Conference on High-Speed Photography (Moscow, 1960), Usp. nauchn. fotogr. (Advances in Scientific Photography), Vol. 9.

[8] S. I. Andreev and M. P. Vanyukov, ZhTF **31**, 961 (1961), Soviet Phys. Technical Physics **6**, 700 (1962).

[9] A. A. Babushkin, JETP **15**, 32 (1945).

[9a] Balashov, Vanyukov, Muratov, and Nilov, Opt. i spektr. **10**, 540 (1961), Optics and Spectroscopy **10**, 279 (1961).

[10] E. J. G. Beeson and K. M. H. Rhodes, J. Photogr. Sci. **4**, 54 (1956).

[11] Bird, Miehe, and Edgerton, Photogr. Engng. **7**, 26 (1956).

[12] W. R. Blevin, Austral. J. Phys. **6**, 203 (1953).

[13] S. Ya. Bogdanov and K. S. Vul'fson, DAN SSSR **30**, 309 (1941).

[14] S. Ya. Bogdanov and K. S. Vul'fson, DAN SSSR **40**, 431 (1943).

[15] W. S. Boyle, J. Appl. Phys. **26**, 584 (1955).

[16] S. I. Braginskiĭ, JETP **34**, 1548 (1958), Soviet Phys. JETP **7**, 1068 (1958).

[17] K. Buss, Arch. Elektrotechn. **26**, 266 (1932).

[18] J. van Calker, Naturwiss. **40**, 434 (1953).

[19] F. E. Carlson and D. A. Pritchard, Illum. Engng. **42**, 235 (1947).

[20] W. D. Chesterman and D. R. Glegg, 2nd Congr. Intern. Photogr. Cinematogr. Ultra-Rapides, Dunod, Paris, 1956, p. 8.

[21] M. Cloupeau, 3rd Congr. Intern. fenom. d'ionniz. gas, Rendiconti, Milano, 1957, p. 196.

[22] M. Cloupeau, Compt. rend. **244**, 2033 (1957).

[22a] M. Cloupeau, J. phys. et radium **21**, 189 (1960).

[23] J. D. Cobine and E. E. Burger, J. Appl. Phys. **26**, 895 (1955).

[24] J. D. Cobine and C. J. Gallagher, Phys. Rev. **74**, 1954 (1948).

[25] W. M. Conn, JOSA **41**, 445 (1951).

[26] W. M. Conn, Z. angew. Phys. **7**, 539 (1955).

[27] K. D. Craig and J. D. Craggs, Proc. Phys. Soc. **B66**, 500 (1953).

[28] J. D. Craggs and J. M. Meek, Proc. Roy. Soc. **A186**, 241 (1946).

[29] J. D. Craggs and J. M. Meek, Research **4**, 4 (1951).

[30] E. David, Z. Phys. **150**, 162 (1958).

[31] G. G. Dolgov and S. L. Mandel'shtam, JETP **24**, 691 (1953).

[32] S. I. Drabkina, JETP **21**, 473 (1951).

[33] H. S. Dunkerley and D. L. Schaefer, J. Appl. Phys. **26**, 1384 (1955).

[34] H. E. Edgerton, JOSA **36**, 390 (1946).

[35] H. E. Edgerton, JSMPE **52**, No. 3, pt. II, 8 (1943).

[36] H. E. Edgerton, Electronic Equipment Engng. (1958).

[37] H. E. Edgerton, 4. Kongr. Intern. Kurzzeitphotographie, Helwich, Darmstadt, 1959, p. 91.

[38] Edgerton, Tredwell, and Cooper, JSMPTE **70**, 177 (1961).

[39] Edgerton, Bonazoli, and Lamb, JSMPTE **63**, 15 (1954).

[40] H. E. Edgerton and P. Y. Cathou, Rev. Sci. Instr. **27**, 821 (1956).

[41] H. E. Edgerton and D. A. Cahlander, JSMPTE **70**, 7 (1961).

[42] A. von Engel and A. E. Robson, J. Appl. Phys. **29**, 734 (1959).

[43] Exploding Wires, Ed. by W. G. Chace, H. K. Moore, Plenum Press, N. Y.—Chapman, London, 1959.

[44] Fabrikant, Safraĭ, and Aronovich, ZhTF **6**, 1006 (1936).

[44a] H. Feldkirchnes and H. Krempl, Arch. Eisenhüttenwesen **27**, 621 (1956).

[45] H. Fischer, JOSA **43**, 394 (1953).

[46] H. Fischer, Phys. Verhandl. **6**, 177 (1955).

[47] H. Fischer, JOSA **47**, 981 (1957).

[48] H. Fischer, Tele-Tech. and Electronics, London **15**, 15 (1956).

[49] H. Fischer, Confer. Extremely High Temperatures, J. Wiley, N.Y.—Chapman, London, 1958, p. 11.

[50] H. Fischer, US Patent, cl. 315-61, No. 2911561, 11.3.1959.

[50a] H. Fischer, JOSA **51**, 543 (1961).

[51] Fitzpatrick, Hubbard, and Thaler, J. Appl. Phys. **21**, 1269 (1950).

[52] N. H. Fletcher and J. M. Somerville, Brit. J. Appl. Phys. **7**, 419 (1956).

[53] R. C. Fletcher, Phys. Rev. **76**, 1501 (1949).

[54] J. W. Flowers, Phys. Rev. **64**, 225 (1943).

[54a] R. L. Forgacs, IRE Nat. Convent. Res. 5, 114 (1957).
[55] G. Frind, Z. angew. Phys. 12, 231 (1960).
[56] K. D. Froome, Proc. Phys. Soc. 60, 424 (1948).
[57] K. D. Froome, Proc. Phys. Soc. B62, 805 (1949).
[58] K. D. Froome, Proc. Phys. Soc. B63, 377 (1950).
[59] F. Früngel, Optik 3, 128 (1948).
[60] F. Früngel, Z. angew. Phys. 5, 102 (1953).
[61] F. Früngel, Z. angew. Phys. 6, 183 (1954).
[62] F. Früngel and W. Thorwart, V.D.I. Zs. 97, 1305 (1955).
[63] N. M. Gegechkori, JETP 21, 493 (1951).
[63a] A. A. Gershun, Phys. Z. Sowjetunion 2, 149 (1932).
[64] G. Glaser, Optik 7, 33, 61 (1950).
[65] G. Glaser, Z. Naturforsch. 6a, 706 (1951).
[66] G. Glaser, Elektron in Wissenschaft und Technik 1951, p. 317.
[67] G. Glaser, Z. Phys. 143, 44 (1955).
[68] H. Grabner and M. Reger, Techn.-Wiss. Abh. Osram. 7, 52 (1958).
[68a] I. M. Gurevich, Zh. opt.-mekh. prom. (Journal of the Optical-Mechanical Industry) No. 4 (1954).
[69] S. D. Gvozdover, JETP 7, 867 (1937).
[70] V. Hermoch, Czech. Phys. J. 9, 84, 221, 377, 505 (1959).
[70a] Hess, Kischel, Morgenroth, and Seliger, Ann. Phys. (7), 8, 189 (1961).
[71] J. B. Higham and J. M. Meek, Proc. Phys. Soc. B63, 649 (1950).
[72] K. Höcker and P. Schulz, Z. Naturforsch. 4a, 266 (1949).
[73] C. D. Hoyt and W. W. McCormick, JOSA 40, 658 (1950).
[73a] W. Jaedicke, ETZ 13, 481 (1961).
[74] V. P. Ivanov and I. S. Marshak, PTÉ No. 1, 92 (1960).
[74a] Kerns, Kirsten, and Cox, Rev. Sci. Instr. 30, 31 (1959).
[75] M. Keilhacker, Z. angew. Phys. 12, 49 (1960).
[76] Kirsanov, Marshak, Razumtsev, and Shchukin, Svetotekhnika (Illumination Engineering), 1962 (in press).
[76a] Kirsanov, Gavanin, and Marshak, Opt. i spektr. 13, 276 (1962), Optics and Spectroscopy 13, 153 (1962).
[76b] Kirsanov, Marshak, and Epshtein, ibid. 13, 442 (1962), transl. p. 244.
[77] G. Knott, Photogr. J. B89, 46 (1949).
[78] W. Kohrmann, 3rd Congr. Intern. fenom. d'ionniz. gas, Rendiconti, Milano, 1957, p. 544.
[79] A. C. Kolb, Phys. Rev. 107, 354 (1957).
[80] V. S. Komel'kov and D. S. Parfenov, DAN SSSR 111, 1215 (1956), Soviet Phys. Doklady 1, 769 (1957).
[81] H. A. Kramers, Philos. Mag. 46, 836 (1923).
[82] W. Krug, Z. techn. Phys. 30, 377 (1937).
[83] J. Krutzsch, ETZ 40, 607 (1928).
[84] B. Kühn, Ann. d. Phys. (7) 3, 241 (1959).
[85] Kvartskhava, Plyutto, Chernov, and Bondarenko, JETP 30, 42 (1956), Soviet Phys. JETP 3, 40 (1956).
[86] M. Laporte, Rev. d'optique 12, 21 (1933).
[87] M. Laporte, J. phys. et radium 8, 340 (1937).
[88] M. Laporte, Compt. rend. 204, 1559 (1937).
[89] M. Laporte, Compt. rend. 209, 95 (1939).
[90] M. Laporte, Les lampes a éclairs lumière blanche et leurs applications, Gauthier-Villars, Paris, 1949.
[91] G. W. le Compte and H. E. Edgerton, J. Appl. Phys. 27, 1427 (1956).
[92] T. H. Lee, J. Appl. Phys. 28, 920 (1957).
[93] T. H. Lee, J. Appl. Phys. 29, 734 (1958).
[94] T. H. Lee, J. Appl. Phys. 30, 166 (1959).
[95] R. Legros, Compt. rend. 234, 718, 1047 (1952).
[96] R. Lehmann, Kino-Technik, No. 3, 81 (1960).
[97] F. Llewellyn Jones, Nature 157, 371, 480 (1946).
[98] F. Llewellyn Jones, Brit. J. Appl. Phys. 1, 60 (1950).
[99] F. Llewellyn Jones, Repts. Progr. Phys. 16, 254 (1953).
[100] I. Sh. Libin, Radiotekhnika i elektronika (Radio Engineering and Electron Physics) 4, 1026 (1959).
[101] F. Logan and H. E. Edgerton, Photograph. Engng. 6, 110 (1955).
[102] A. Lompe, Lichttechnik 10, 108 (1958).
[103] A. Lompe, Elektrizitätsverw. 33, 283 (1958).
[104] J. S. T. Looms and R. J. North, 3rd Intern. Congr. High-Speed Photogr., Butterworth, London, 1957, p. 62.
[105] J. C. Lowson, IES Lighting Rev. 20, 114 (1958).
[106] A. A. Mak, DAN SSSR 123, 671 (1958), Soviet Phys. Doklady 3, 1266 (1959).
[107] A. A. Mak, Opt. i spektr. 8, 278 (1960), Optics and Spectroscopy 8, 145 (1960).
[108] A. A. Mak, Investigation of the Radiation of an Intense Spark Discharge. Dissertation (State Optics Institute, 1960).
[109] A. A. Mak, ZhTF 31, 94 (1961), Soviet Phys. Technical Physics 6, 67 (1961).
[110] M. McChesney and J. D. Graggs, J. Electronics and Control 4, 481 (1958).
[111] J. H. Malmberg, Rev. Sci. Instrum. 26, 1027 (1957).
[112] S. L. Mandel'shtam and N. K. Sukhodrev, JETP 24, 701 (1953).
[113] S. L. Mandel'shtam and N. K. Sukhodrev, Izv. AN SSSR ser. fiz. 19, 11 (1955), Columbia Tech. Transl. p. 7.
[114] Mandel'shtam, Sukhodrev, and Shabanskiĭ, Materials of the Tenth All-Union Conference on Spectroscopy, Vol. II, published by L'vov University, 1957, page 148.
[115] S. L. Mandel'shtam and I. P. Tindo, Izv. AN SSSR ser. fiz. 19, 60 (1955), Columbia Tech. Transl. p. 57.
[116] S. Mandelstam, 3rd Congr. Intern. fenom. d'ionniz. gas, Rendiconti, Milano, 1957, p. 695.
[117] I. S. Marshak, Electric Breakdown in Gas at Atmospheric Pressure, Dissertation (Moscow Power Institute, 1945).

[118] I. S. Marshak, JETP **16**, 703, 718 (1946).
[119] I. S. Marshak, Collection of Materials on Vacuum Technology, Vol. 7, Moscow, Gosenergoizdat, 1955, page 3.
[120] I. S. Marshak, Svetotekhnika (Illumination Engineering) No. 1, 17 (1956).
[121] I. S. Marshak, 3rd Congr. Intern. High-Speed Photogr., Butterworth, London, 1957, p. 30.
[122] I. S. Marshak, Svetotekhnika (Illumination Engineering) No. 1, 17 (1957).
[123] I. S. Marshak, PTÉ, No. 5, 3 (1957).
[124] I. S. Marshak, Svetotekhnika (Illumination Engineering) No. 6, 22 (1957).
[125] I. S. Marshak, ibid. No. 6, 17 (1959).
[126] I. S. Marshak, UFN **71**, 631 (1960), Soviet Phys. Uspekhi **3**, 624 (1961).
[127] I. S. Marshak, Collection of Materials on Vacuum Technology, Vol. 22, Moscow, Gosenergoizdat, 1960, page 27.
[128] I. S. Marshak, Opt. i spektr. **10**, 801 (1961), Optics and Spectroscopy **10**, 424 (1961).
[128a] I. S. Marshak, PTÉ, No. 3, 5 (1962).
[129] Marshak, Vasil'ev, Mironova, Ivanov, and Vdovchenko, Usp. nauchn. fotogr. (Advances in Scientific Photography) **6**, 43 (1959).
[130] Marshak, Vasil'ev, Tokhadze, and Rogatin, Svetotekhnika (Illumination Engineering) No. 4, 8 (1961).
[130a] Marshak, Vasil'ev, and Vasserman, ibid. No. 3, 7 (1962).
[131] I. S. Marshak and L. I. Shchukin, JSMPTE **70**, 169 (1961).
[132] I. S. Marshak and V. A. Subbotin, Collection of Materials on Vacuum Technology, Vol. 13, Moscow, Gosenergoizdat, 1957, pp. 12, 28.
[133] B. Meyer, Z. angew. Phys. **5**, 139 (1953).
[134] Mezhueva, Stekol'nikov, and Efendiev, ZhTF **20**, 308 (1950).
[135] J. W. Mitchel, Trans. Ill. Engng. Soc. **14**, 91 (1949).
[136] I. Sh. Model', JETP **32**, 714 (1957), Soviet Phys. JETP **5**, 589 (1957).
[137] F. L. Mohler, Nat. Bur. Stand. J. Res. **21**, 873 (1938).
[138] Morgenroth, Hess, Kischel, and Seliger, Ann. Physik (7), **8**, 175 (1961).
[139] W. Müller, Z. Phys. **149**, 397 (1957).
[140] P. M. Murphy and H. E. Edgerton, J. Appl. Phys. **12**, 848 (1941).
[141] E. B. Noel and P. B. Davies, Photogr. Sci. and Techn. **1**, 11 (1950).
[141a] P. Nolan, JSMPTE **70**, 632 (1961).
[142] N. N. Ogurtsova and I. V. Podmoshinskii, Opt. i spektr. **4**, 539 (1958).
[143] N. N. Ogurtsova, Opt.-mekh prom. (Optical-Mechanical Industry) No. 1, 1 (1960).
[144] F. Ollendorf, Arch. Elektrotechn. **26**, 193 (1932).
[145] F. Ollendorf, Arch. Elektrotechn. **27**, 169 (1933).
[146] Olsen, Edmonson, and Gayhart, J. Appl. Phys. **23**, 1157 (1952).
[147] G. V. Ovechkin, Materials of the Tenth All-Union Conference on Spectroscopy, Vol. I, published by L'vov University, 1957, page 365.
[148] P. C. L. Pfeil and L. B. Griffiths, Nature **183**, 1481 (1959).
[149] G. Porter, Proc. Roy. Soc. **A200**, 284 (1950).
[150] G. Porter and E. R. Wooding, J. Sci. Instrum. **36**, 147 (1959).
[151] S. M. Raĭskiĭ, JETP **10**, 908 (1940).
[152] S. M. Raĭskiĭ, JETP **18**, 941 (1948).
[153] C. Ramsauer and R. Collath, UFN **14**, 957 (1934) and **15**, 407 (1935).
[154] N. W. Robinson, Philips Techn. Rev. **16**, 13 (1954).
[155] A. E. Robson and A. von Engle, Nature **175**, 646 (1955).
[156] Rogowski, Flegler, and Tamm, Arch. Elektrotechn. **18**, 479 (1927).
[157] W. Rogowski and R. Tamm, Arch. Elektrotechn. **20**, 107 (1928).
[158] W. Rogowski, Phys. Z. **33**, 797 (1932).
[159] W. Rogowski, Z. Phys. **100**, 1 (1936).
[160] R. Rompe and P. Schulz, Z. Phys. **6**, 105 (1941).
[161] E. Rose, Ann. d. Phys. (7) **4**, 15 (1959).
[162] E. K. Zavoĭskii and S. D. Fanchenko, DAN SSSR **100**, 661 (1955).
[163] H. Schirmer, Z. Phys. **156**, 55 (1959).
[164] H. Schirmer and J. Friedrich, Techn. Wiss. Abhandl. Osram **7**, 11 (1958).
[165] W. Schmidt and R. Lehmann, Light and Lighting **52**, 24 (1959).
[166] Shao Chi Lin, J. Appl. Phys. **25**, 54 (1954).
[167] L. I. Sedov, DAN SSSR **47**, 94 (1945).
[168] L. I. Sedov, Prikl. matem. i mekh. (Applied Mathematics and Mechanics) **10**, 241 (1946).
[169] V. M. Zimin, Materials of Tenth All-Union Conference on Spectroscopy, Vol. II, published by L'vov University, 1957, page 161.
[170] A. S. Zingerman, ZhTF **26**, 1015 (1956), Soviet Phys. Tech. Phys. **1**, 992 (1957).
[171] A. S. Zingerman and D. A. Kaplan, ZhTF **29**, 877 (1959), Soviet Phys. Tech. Phys. **4**, 792 (1960).
[172] W. R. Sittner and E. R. Peck, JOSA **39**, 474 (1949).
[173] N. N. Sobolev, JETP **13**, 137 (1945).
[174] N. N. Sobolev, JETP **17**, 986 (1947).
[175] J. M. Somerville and W. R. Blevin, Phys. Rev. **76**, 982 (1949).
[176] Somerville, Blevin, and Fletcher, Proc. Phys. Soc. **B65**, 963 (1952).
[177] J. M. Somerville and N. H. Fletcher, Brit. J. Appl. Phys. **7**, 419 (1956).
[178] J. M. Somerville and C. T. Grainger, Brit. J. Appl. Phys. **7**, 109, 400 (1956).
[179] J. M. Somerville and J. F. Williams, Proc. Phys. Soc. **76**, 309 (1959).

[179a] H. Späth and H. Krempl, Z. angew. Phys. **12**, 8 (1960).
[180] W. R. Stamp and R. P. Coghlan, JSMPTE **62**, 105 (1954).
[181] C. C. Suits, Gen. Electr. Rev. **39**, 430 (1936).
[181a] N. K. Sukhodrev and S. L. Mandel'shtam, Opt. i spektr. **6**, 723 (1959).
[182] G. Taylor, Proc. Roy. Soc. **A201**, 159 (1950).
[183] M. Tëpler, Arch. Elektrotechn. **18**, No. 6 (1927).
[184] D. P. C. Thackeray, 3rd Intern. Congr. High-Speed Photogr., Butterworth, London, 1957, p. 21.
[185] D. P. C. Thackeray, J. Sci. Instr. **35**, 206 (1958).
[186] Tuttle, Brown, and Whitemore, Photo-Technique, September, 1940, p. 52.
[187] F. A. Charnaya, Opt. i spektr. **1**, 857 (1956).
[188] F. A. Charnaya, Opt. i spektr. **4**, 725 (1958).
[189] F. A. Charnaya, Investigation of Optical Characteristics of Flash Lamps of High Pressure, Dissertation (Moscow Power Institute, 1960).
[190] F. A. Charnaya, Svetotekhnika (Illumination Engineering) No. 10, 13 (1960).
[191] A. Unsöld, Physik der Sternatmosphären, 2. Aufl., Springer, Berlin, 1955.
[192] Vaĭnshteĭn, Leontovich, Malyavkin, and Mandel'shtam, JETP **24**, 326 (1953).
[193] M. P. Vanyukov, ZhTF **16**, 889 (1946).
[194] M. P. Vanyukov, Zh. opt.-mekh. prom. (Journal of Optical-Mechanical Industry) No. 6, 9 (1953).
[195] M. P. Vanyukov and Khazanov, ibid. No. 2, 6 (1953).
[196] M. P. Vanyukov and V. I. Isaenko, Svetotekhnika (Illumination Engineering) No. 3, 7 (1960).
[197] Vanyukov, Isaenko, and Khazov, ZhTF **25**, 1248 (1955).
[198] M. P. Vanyukov and A. A. Mak, Opt. i spektr. **1**, 642 (1956).
[199] M. P. Vanyukov and A. A. Mak, UFN **66**, 301 (1958), Soviet Phys. Uspekhi **1**, 137 (1959).
[200] M. P. Vanyukov and A. A. Mak, DAN SSSR **123**, 1022 (1958), Soviet Phys. Doklady **3**, 1268 (1959).
[201] M. P. Vanyukov and A. A. Mak, Izv. AN SSSR ser. fiz. **23**, 962 (1959), Columbia Tech. Transl. p. 951.
[202] M. P. Vanyukov and A. A. Mak, Paper delivered at Second All-Union Conference on High Speed Photography (see [7]).
[203] Vanyukov, Mak, and Muratov, Opt. i spektr. **6**, 17 (1959).
[204] Vanyukov, Mak, and Muratov, ibid. **8**, 439 (1960), Translation p. 233.
[204a] Vanyukov, Mak, and Sadykova, DAN SSSR **135**, 577 (1960), Soviet Phys. Doklady **5**, 1334 (1961).
[205] Vanyukov, Mak, and Ures, Opt. i spektr. **4**, 19 (1958).
[205a] Vanyukov, Muratov, and Mukhitdinova, Opt. i spektr. **10**, 561 (1961), Optics and Spectroscopy **10**, 294 (1961).
[205b] N. Warmoltz and A. Helmer, Philips Techn. Rundsch. **10**, 183 (1948).
[206] Vasil'ev, Kirsanov, Levchuk, and Marshak, Collection of Materials on Vacuum Technology, Vol. 24, Moscow, Gosenergoizdat, 1960, page 43.
[207] Vasil'ev, Levchuk, and Marshak, Opt. i spektr. **11**, 118 (1961), Optics and Spectroscopy **11**, 61 (1961).
[207a] V. I. Vasil'ev and I. S. Marshak, Collection of Materials on Vacuum Technology, Vol. 14, Moscow, Gosenergoizdat, 1958, page 19.
[208] Vdovchenko, Marshak, and Nikol'skaya, Collection of Materials on Vacuum Techniques, Vol. 21, Moscow, Gosenergoizdat 1955, page 17.
[209] W. Weizel, Z. Phys. **135**, 639 (1953).
[210] W. Weizel, Appl. Sci. Res. **5**, 277 (1955).
[211] W. Weizel and R. Rompe, Ann. d. Phys. **1**, 285 (1955).
[212] W. Weizel and R. Rompe, Theorie elektrischer Lichtbogen und Funken, Barth, Leipzig, 1949.
[213] L. Weltner, Z. Phys. **136**, 631 (1953).
[213a] B. M. Vodovatov and M. I. Épshteĭn, Usp. nauchn. fotogr. (Progress in Scientific Photography) **6**, 35 (1959).
[214] J. Wrana, Arch. Elektrotechn. **33**, 656 (1939).
[215] K. S. Vul'fson, Elektrichestvo (Electricity), No. 11, 16 (1946).
[216] K. F. Vul'fson and I. Sh. Libin, JETP **21**, 510 (1951).
[217] Vul'fson, Libin, and Charnaya, Izv. AN SSSR ser. fiz. **19**, 61 (1955), Columbia Tech. Transl. p. 58.
[218] K. S. Vul'fson and F. A. Charnaya, Materials of the Tenth All-Union Conference on Spectroscopy, Vol. II, published by L'vov University 1957, p. 73.
[219] Zhil'tsov, Marshak, and Shchukin, Svetotekhnika (Illumination Engineering), No. 11, 13 (1961).
[220] E. Zizka, Czechoslovak Phys. J. **10**, 327 (1960).

Translated by J. G. Adashko